OPEN ACCESS

Review Article

Current oncologic concepts and emerging techniques for imaging of head and neck squamous cell cancer

Abstract

The incidence of head and neck squamous cell carcinoma (HNSCC) is increasing and currently they account for 5% of all malignancies worldwide. Inspite of ongoing developments in diagnostic imaging and new therapeutic options, HNSCC still represents a multidisciplinary challenge.

One of the most important prognostic factors in HNSCC is the presence of lymph node metastases. Patients with confirmed nodal involvement have a considerable reduction of their 5-year overall survival rate. In the era of individually optimised surgery, chemotherapy and intensity modulated radiotherapy, the main role of pre- and posttherapeutic imaging remains cancer detection at an early stage and accurate follow-up. The combined effort of early diagnosis and close patient monitoring after surgery and/or radio-chemotherapy influences disease progression and outcome predicition in patients with HNSCC.

This review article focuses on currrent oncologic concepts and emerging tools in imaging of head and neck squamous cell cancer. Besides the diagnostic spectrum of the individual imaging modalities, their limitations are also discussed. One main part of this article is dedicated to PET-CT which combines functional and morphological imaging. Furthermore latest developments in MRI are presented with regard to lymph node staging and response prediction. Last but not least, a clinical contribution in this review explains, which information the head and neck surgeon requires from the multimodality imaging and its impact on operation planning.

Keywords: HNSCC, head and neck carcinoma, PET-CT, hypoxia imaging, diffusion weighted imaging, MRI, lymph node staging

Maliha Sadick[1]
Stefan O. Schoenberg[1]
Karl Hoermann[2]
Haneen Sadick[2]

1 Institute of Clinical Radiology and Nuclear Medicine, University Hospital Mannheim, Medical Faculty Mannheim of the University of Heidelberg, Mannheim, Germany

2 Department of ORL and Head and Neck Surgery, University Hospital Mannheim, Medical Faculty Mannheim of the University of Heidelberg, Mannheim, Germany

1 Introduction

1.1 General overview

Head and Neck Squamous Cell Carcinoma (HNSCC) is the most common tumor entity in the head and neck region. It mainly originates from the mucosal space, which extends from the skull base to the proximal esophagus. The head and neck region is subdivided in the oral cavity, pharynx and larynx [1]. The pharyngeal space contains the nasopharynx, oropharynx and hypopharynx and includes the tonsils, the floor of the mouth and the soft palate. Malignancies of the floor of the mouth and the oropharynx can usually be diagnosed clinically and endoscopically because of their superficial anatomical location. In laryngeal carcinoma, which is the most common HNSCC, tumor spread and lymph node status should be assessed with cross sectional imaging, as diagnosis can not be reliably based on clinical examination alone [2].

Treatment of HNSCC currently considers multimodal therapy concepts combining surgery with radio-chemotherapy [2]. Especially in advanced tumor stages, where surgical resection is not feasible, radio-chemotherapy is an established treatment [3], [4]. Inspite of improved tumor detection and multimodal treatment concepts, 5-year overall survival according to the current literature is usually less than 50% in patients with HNSCC [2]. Pretherapeutic tumor staging in HNSCC must consider tumor spread and extension, detection of lymph node metastases and assessment of a potentional vascular infiltration, either by the tumor itself or by suspicious lymph nodes. Usually after clinical and endoscopic examination, imaging is performed and contributes to staging, therapy planning and patient follow-up [5], [6]. Current treatment concepts are in favour of therapeutic procedures that combine established chemotherapeutic agents with anti-angiogenic substances like Cetuximab [6]. In this setting, clinical and image guided evaluation of tumor volume and its localization, as well as assessment of cervical lymph node spread and angioinvasion are fundamental for optimising therapy options. Close posttherapeutic patient monitoring is equally essential for improved patient outcome. It should be performed in the first two years after diagnosis of HNSCC in order to identify and treat potential tumor recurrence in the initial stage.

Patients' prognosis is undoubtedly affected by delayed diagnosis, taking into consideration that more than 50% of patients already present with advanced tumor stages. This includes clinical obvious lymph node swelling, swallowing disorder, pain in the oropharynx and hoarseness. For tumor stage adjusted therapy planning, special requirements need to be fulfilled by diagnostic imaging. The established TNM-classification and the neck level classification of lymph nodes according to Robbins are fundamental for the staging of HNSCC [7].
In this review, the diagnostic impact of computed tomography (CT), magnetic resonance imaging (MRI) and positron emission tomography-computed tomography (PET-CT) on oncologic imaging of HNSCC is characterised. Due to the rare incidence of carcinomas of the nasal cavity and the sinuses, between 0.2 and 0.8%, these tumors will not be considered in this review article [1], [2].

1.2 Tumor epidemiology

The incidence of HNSCC is increasing with approximately 650,000 cases annually. In men, HNSCC is five times more common than in women. In Europe mainly patients at the age of 50 to 60 years are affected [8]. Head and neck squamous cell carcinomas account for 2 to 4% of all malignancies worldwide. Whereas in male squamous cell carcinomas of the larynx, oro- and hypopharynx are predominant, in female mainly HNSCC of the oral cavity and the oropharynx is diagnosed [2]. The high incidence of HNSCC is induced by excessive nicotine and alcohol abuse [9]. These exogenic risk factors trigger a dose-effect dependant chronic inflammation of the oral mucosa and therefore represent a precancerous lesion which is responsible for the induction of HNSCC [10]. The human papillomavirus (HPV) is associated with the development of carcinomas of the oral cavity and the pharynx. The Epstein-Barr virus (EBV) is commonly associated with nasopharyngeal cancer, which is very rare in Europe with an incidence of 0.2% compared to 18% in Asia [11]. Nasopharyngeal carcinomas, unlike HNSCC, are characterized by a submucosal growth which is not easily accessible by surgery. Previous exposure to EBV can induce nasopharyngeal carcinoma which resembles squamous cell carcinoma of an undifferentiated type, which is radiosensitive. In case of early initiation of radiotherapy, a 5 year overall survival rate up to 70% is achieved [11].
Endogenic factors like patient age and genetic predisposition also contribute towards tumor development, as with age the exposure to cancerogenic factors might increase. The presence of a p53 gene mutation can trigger HNSCC in young adults between 30 and 40 years of age [12], [13].

1.3 Current prognostic factors

Diagnosis, therapy and follow-up of HNSCC require an intensive multidisciplinary cooperation between head and neck surgeons, radiologists, radiotherapists and oncologists, as the current 5 year overall survival rate in the affected patients is yet very poor with only 42 to 48% [14]. Tumor size, infiltration depth and histological tumor type correlate with the degree of tumor invasion into anatomical structures. Therefore tumor resection grade and tumor free margins represent (R0-resection: resection for cure or complete remission, R1-resection: macroscopic tumor resection, microscopic residual tumor, R2-resection: macroscopic residual tumor) essential prognostic factors [14], [15]. Lymphatic drainage as well as the pattern of lymph node involvement very much depend on the location of the primary tumor. The classification of malignant lymph nodes according to size, ipsi- and/or contralateral spread and distant metastases, which preferably occur in the lung and pleura in HNSCC, have to be taken into consideration, too [7], [15]. Other factors that influence the course of disease and patient survival, are age, sex, general condition and comorbidities of the patient.
Presently no reliable prognostic markers for response-evaluation in HNSCC are available. The expression of molecular markers in lymph node metastases is currently under investigation. In order to deliver anti-angiogenic targeted therapy to the tumor, the expression of epithelial and endothelial proliferation markers in lymph node metastases is being validated in several studies at the moment [16], [17], [18]. Therefore PET-CT plays a key role in predicition of recurrence-free survival of the patients, as alterations of the SUV value in lymph node metastases after induction chemotherapy is a reliable prognosis marker [19]. Another advantage of PET-CT in diagnosis and follow-up of HNSCC is the fact that it can distinguish between tumor recurrence and remaining rest tumor after therapy.

2 Computed tomography

2.1 Status of multidetector-computed tomography for diagnosis and differential diagnosis of head and neck cancer

The most commonly applied cross-sectional imaging modality for preoperative assessment and posttherapeutic follow-up of HNSCC is multidetector-computed tomography (MD-CT) [20]. The establishment of multidetector technology has resulted in improved spatial resolution in z-axis with partial volume effects becoming insignificant. Two x-ray tubes coupled to a detector system in one gantry, at an angle of 90°, enable rapid and multidimensional coverage of the volume of interest. Especially patients with advanced tumor stages and reduced compliance due to dyspnea and swallowing disorder, benefit from the increased speed of CT examination. Short CT scan times and reduced motion artifacts improve the diagnostic output of CT. Whereas MD-CT offers narrow slice collimation up to 0.6 mm and multiplanar reconstructions, two factors which are optimally suited for imaging

of bony structures, MRI is the best choice for imaging soft-tissue lesions. MD-CT provides reduced scan time combined with short patient gantry exposure time and is therefore well suited for whole body staging and exclusion of distant metastases in oncologic cases [21].

Patients who present with lymph node stages N2 or N3 at the time of diagnosis, very often already have distant metastases or are likely to develop osseous and pulmonary metastases in 84% within 2 years [21]. In these cases tumor therapy mainly comprises of surgical tumor debulking followed by systemic chemotherapy. Detection of distant metastases is sensitively and specifically performed with MD-CT (see Figure 1) and can be used as a prediction marker for the recurrence-free survival of the patients. Widespread overall availability of MD-CT in many clinical centers make it an ideal diagnostic tool for preoperative and posttherapeutic imaging after neck dissection, reconstructive surgery or radio-chemotherapy in order to differentiate between postsurgical scar and tumor recurrence [22], [23].

Established scan protocols for evaluation of HNSCC, regardless of the manufacturer, recommend biphasic CT in arterial and portalvenous phase. The patient should be positioned in supine position, with both arms placed bellow the chest and lateral to the abdomen. The application of 80 to 100 ml of iv contrast is usually sufficient for thin-slice data sets of the head and neck region including multiplanar sagittal and coronal image reconstructions. The selection of 0.6 and 1.0 mm collimations enable high quality image reconstructions as well as virtual CT endoscopies of the head and neck region. Scanning should be performed from the skull base to the tracheal bifurcation with focus on the extension of the primary tumor and the cervical lymph node status. Coronal CT planes enable the assessment of vascular involvement and arterial or venous infiltration by the tumor itself or by lymph node metastases. In contrast to MRI, radiation exposure, application of iodine containing contrast agents and dental metallic artefacts are limitations of MD-CT.

MRI is valuable for the diagnosis of a potential skull base infiltration in oropharyngeal and nasopharyngeal cancer, whereas CT is prefered for the evaluation of cancer of the hypopharynx and larynx [23]. In patients with HNSCC of the oral cavity with potential involvement of the tonsils, the base of the tongue and the floor of the mouth, MD-CT can reliably assess infiltration of the mandible. After all, the diagnosis of osseous metastases with osteolysis of the mandible, like demonstrated in a patient with stage T3N2M1 cancer of the floor of the mouth, can alter treatment decisions in favour of radio-chemotherapy (see Figure 2a and b). MD-CT has a sensitivity of 50% and a specificity of almost 100% for the detection of osteodestruction in HNSCC [24]. In contrast to MRI, MD-CT can sensitively and specifically evaluate vascular encasement and infiltration as well as infiltration of the prevertebral space and mediastinum and a perineural spread into the skull base, which are all potential signs of inoperability [25]. Ultimately, the head and neck surgeon has to decide whether tumor resectability is possible, depending on the patients clinical condition and imaging findings (see Figure 2c and d).

Many authors consider computed tomography to be the most sensitive tool for imaging the larynx with regard to inflammatory and malignant findings [26], [27]. Polyps of the vocal cords and laryngeal papillomas can be diagnosed by virtual, CT-assisted laryngoscopy with high sensitivity but little specificity [25]. Endoscopy and biopsy are the methods of choice for investigation of laryngeal carcinoma, although tumors with invasion of the pre-epiglottic and para-epiglottic space often demonstrate submucosal spread and can therefore not be easily detected by endoscopy. In these cases MD-CT is recommended for operation planning, as it provides valuable information on localisation, size and depth of tumor extension [25], [26]. Cancer of the vocal cords and the glottic and subglottic space can also be missed easily by endoscopic examination whereas MD-CT shows a sensitivity of up to 93% for lesion detection [26]. The diagnosis of cartilage invasion in laryngeal cancer can be performed sensitively with MD-CT and contributes towards surgery planning with regard to partial or radical laryngectomy [27], [28]. CT imaging criteria for cartilage invasion are lysis, sclerosis and erosions of the cartilage as well as extralaryngeal destruction. These CT criteria have a negative predictive value between 95 and 100%. In case they are not diagnosed on CT, an infiltration of the laryngeal cartilage can be excluded and the patient can benefit from larynx-preserving surgery [28].

Due to its speed, high spatial resolution and low susceptibility artefacts, computed tomography is used for the analysis of tumor perfusion in some centers. Tumor vascularization, depending on the microcapillary density in HNSCC, can be determined using a 2-compartment model [29]. Functional perfusion parameters such as blood volume and blood flow in the tumor are then used for response evaluation after radio-chemotherapy, since cancers with high tumor perfusion rate and correlating high microcapillary density show better response to radiochemotherapy than carcinomas with low tumor vascularisation [29].

While in PET-CT the "standard uptake value" (SUV value) represents a functional and reliable parameter for lymph node determination, CT and MRI use morphologic parameters for the classification of lymph nodes. Several research groups have evaluated the detection of cervical lymph node metastases of HNSCC in PET-CT compared with other cross-sectional imaging modalities [22], [30], [31], [32], [33] [34]. Criteria for malignancy include a maximum transverse diameter of the lymph node greater than 15 mm, cystic and necrotic areas with or without liquefaction, a round-shaped lymph node, cluster formation and an irregular boundary of the lymph node capsule or extra capsular lymph node spread [22], [30], [31], [32], [33], [34]. The results of studies on sensitivity and specificity for the detection of lymph node metastases in PET-CT, CT and MRI are listed in Table 1. Only lymph node excision and subsequent histopathological examination enable reliable assessment of lymph node histology. An

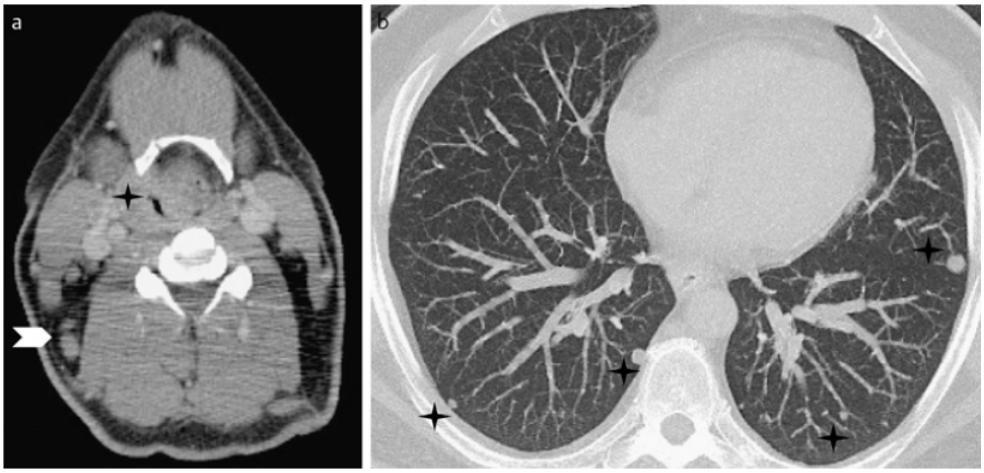

Figure 1: 43-year-old male with T4N2cM1 right sided supraglottic laryngeal cancer (Fig. 1a on the left, black star) and ipsilateral lymph node metastases in the right cervical level III (Fig. 1a on the left, white arrow).
The pulmonary window setting in the axial CT MIP demonstrates at least 4 metastases in segment 6 of both pulmonary lobes (Fig. 1b on the right side, black stars).

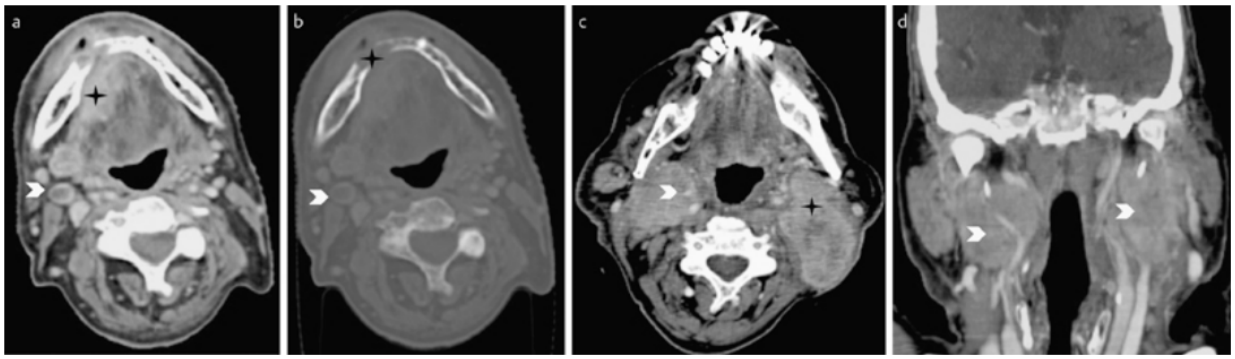

Figure 2: 77-year-old male with T3N2M1 cancer of the floor of the mouth on the right side. The soft tissue window setting in post contrast CT demonstrates an extensive hyperdense tumor with osteodestruction of the mandible (Fig. 2a, black star). Additionally a histologically confirmed lymph node metastases with central necrosis in the right sided cervical level II is visible (Fig. 2a, white arrow).
The bone window setting shows the osteodestruction of the mandible (Fig. 2b, black star).
72-year-old male with T3N3 oropharyngeal cancer. Extensive bilateral neck lymph node metastases with encasement of the carotid artery on both sides (Fig. 2c, white arrow). Coronary CT image reconstruction demonstrates a both sided tumor infiltration of the carotid bifurcation (Fig. 2d, white arrow).

Table 1: Sensitivity and specificity of CT, MRI and PET-CT for detection of cervical lymph node metastases

Author	Year	Sensitivity & Specificity **CT**	Sensitivity & Specificity **MRI**	Sensitivity & Specificity **PET-CT**	Notes
Kau et al. [30]	1999	88%–40%	88%–40%	87%–94%	—
Di Martino et al. [31]	2000	82%–94%	82%–94%	82%–87%	—
Schroeder et al. [32]	2008	69%	39%	54%	for the NO neck in cancer of the oral cavity
Vandecaveye et al. [33]	2009	—	76%–85%	—	diffusion-weighted MRI with ADC maps
Yoon et al. [34]	2009	95%	97%	97%	—
Sham et al. [22]	2011	82%–85%	80%–79%	90%–94%	—

indication for cervical lymph node dissection after previous cross-sectional imaging is given in cases where a malignant lymphoma is suspected, persistent lymphadenopathy is diagnosed with no apparent primary tumor in the head and neck region, lymph node metastases of other primary tumors outside the head and neck region are suspected or an inflammatory systemic disease or vasculitis such as tuberculosis and sarcoidosis must be excluded [34].

In dual-energy CT (DE-CT) 2 X-ray tubes generate two different voltages of 80 kV and 140 kV, so that tissue can be sampled optimally with different absorption spectra. With this technique, high-attenuation artefacts are minimized and noise-reduction as well as improved soft tissue contrast is achieved [35]. Because of these properties, after iv administration of iodinated contrast agent, the iodine content of tumors can be demonstrated and quantified with DE-CT. This approach is promising, because the iodine uptake in tumors or lymphatic tissue may be utilised as a surrogate marker for tumor perfusion and angiogenesis, as demonstrated in a study by Schmid-Bindert et al. in patients with bronchial carcinoma and suspected thoracic lymph node metastases in DE-CT. This study also confirmed a correlation between the iodine uptake in the tumor and the corresponding standard uptake value (SUV) in 18F FDG PET-CT [35].

Short scanning times, objectivity and reproducibility of the CT findings in contrast to sonography, a reduction of motion artefacts by the multi-detector technology and the possibility of secondary multiplanar reconstructions make computed tomography very valuable for the assessment of HNSCC [36]. As a staging tool it is utilised for determining the depth of infiltration of tumors, especially in submucosal spread, and their pattern of metastases. Especially in carcinomas of the oral cavity, the hypopharynx and larynx, where depth of tumor infiltration and a potential infiltration of the bone must be clarified, the impact of contrast-enhanced CT on diagnosis and treatment planning is tremendous.

3 Positron emission tomography-computed tomography

3.1 18 F Fluorodeoxyglucose PET-CT for nodal staging in head and neck cancer and cervical squamous cell cancer of unknown primary (CUP)

Positron emission tomography-computed tomography is a noninvasive imaging modality that combines the functional information of PET with the morphological information of CT and utilises this information for the imaging of tumors with increased glucose metabolism [37]. CT and MRI are established diagnostic procedures for pre-and post-therapeutic imaging of squamous cell carcinoma of the head and neck region. Yet, they can not replace the metabolic information of PET, which can characterize a lymph node irrespective of its morphology. While contrast-enhanced CT and MRI are established imaging modalities for the T classification of head and neck cancer and enable assessment of the primary tumor and its extension along with the clinical and endoscopic findings, PET allows distinction of potential lymph node metastases, depending on their size and FDG activity [37]. Cystic-necrotic lymph node metastases, which occur frequently in cancer of the tonsils, can be diagnosed with an accuracy up to 92% with 18F-FDG PET-CT [38]. Regardless of size and extent of the primary tumor, the localization of lymph node metastases and information on unilateral or bilateral spread is essential for operation planning and definition of radiation field. 18F-FDG PET-CT is a functional imaging method with morphological input and therefore represents a roadmap for tumor therapy (see Figure 3).

The most commonly used PET tracer is the glucose analogon 18 F Fluorodeoxyglucose (18F-FDG). There is an uptake of 18F-FDG by tumor cells and metabolization by hexokinase to FDG-6-phosphate. FDG-6-phosphate accumulates in the cells as it can not be reduced further through glycolysis [39]. The quantitative assessment of the glucose metabolism in these cells is determined by the standard uptake value (SUV). The SUV is defined as the FDG uptake in a tumor over a certain time interval, considering tracer decay, the administered dose of the PET tracer and the patient's weight.

Technical factors, such as equipment, PET-CT calibration and injection mode, as well as physiological factors like blood sugar levels, increased muscle activity and existing inflammation in the body, influence SUV quantification [39]. Increased standard uptake values are physiological in the Waldeyer's ring and in the vocal cords due to coughing or speech. The head and neck region, due to its small-sized anatomical structures, is indeed a diagnostic challenge. The detection of lesions with FDG uptake and assessment of their SUV requires a dedicated examination protocol in order to guarantee optimal diagnostic accuracy of the PET-CT scan. The evaluation of the SUV before and after treatment of HNSCC is an important prognostic marker for determining the individual survival time of patients, as high SUV values are usually associated with high T stage and N1-3 metastases and thus correlate with a shorter tumor-free survival rate of patients compared to low T stages in a N0 or N1 neck [40].

An established examination protocol at our institution recommends body weight-adapted intravenous administration of 250–350 Mega Becquerel (MBq) 18F-FDG after previous fasting of the patient for at least 6 to 8 hours. The whole-body PET-CT is initiated approximately 60 minutes after iv application of the tracer on the Biograph True Point™ HD PET-CT System (Siemens, Healthcare Sector, Erlangen/Germany). Attenuation correction CT is performed with 50–70 mAs, 120 kV, 5 mm slice thickness and 3 mm increment. PET is carried out in the 3D mode. The standard examination parameters, all applied with the True X algorithm, comprise of 3 iterations, 24 subsets, the Gaussian filter 3 mm Full Width Half Maximum (FWHM) for PET raw data reconstruction and a matrix size

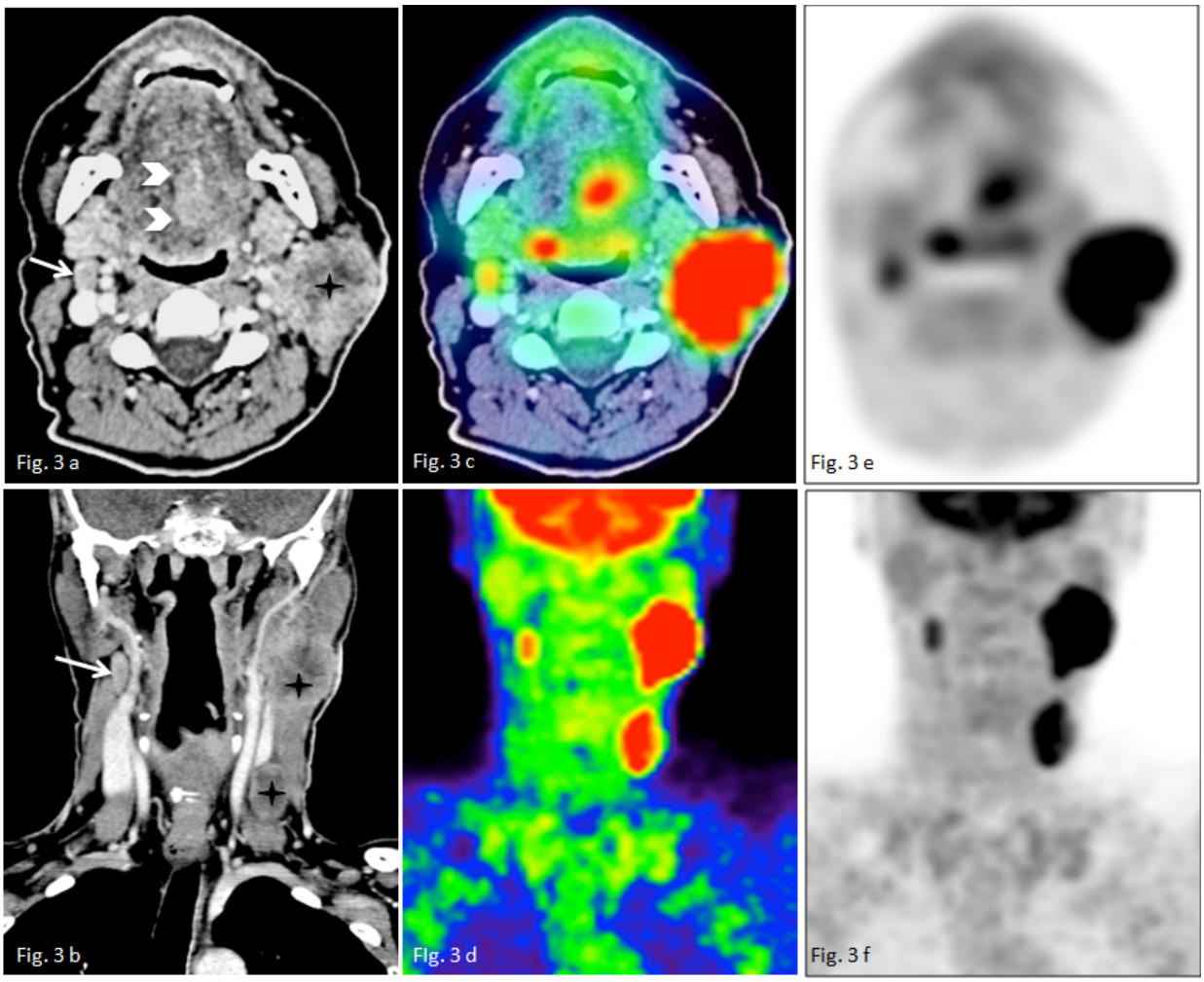

Figure 3: 51-year-old male with diagnosis of a T3N2M0 cancer of the base of the tongue on the left side. Post contrast CT shows a necrotic lymph node metastasis 3 cm in size in the left cervical level II (Fig. 3a, black star). On coronal CT slices lymph node metastases in the left level II and III are visible (Fig. 3b, black star; Fig. 3d and 3f). PET demonstrates intensive FDG uptake by the lymph node metastases (Figure 3e and 3f). A lymph node of 1.5 cm in the right neck level II could not be assessed with CT (Fig. 3a and 3b, white arrow). This lymph node shows intensive FDG Uptake in PET (Fig. 3e and 3f) and the fused axial and coronary PET-CT images (Fig. 3c and 3d). Bicervical neck dissection was performed. Histologically a lymph node metastasis was confirmed.

Intensive contrast agent accumulation in the primary tumor in the left sided base of the tongue (Fig. 3a, 2 white arrows) which correlates with intensive FDG uptake in PET-CT (Fig. 3c and 3e).

of 200x200. All patients then undergo a diagnostic biphasic CT in arterial and portalvenous phase from the skull base to the chest after intravenous administration of 100 ml iodinated contrast agent. The study parameters are standardized to 16x1.2 mm slice thickness and 3 mm increment. PET and CT raw data are reconstructed in multiplanar cross-sections. For image analysis and diagnostic reporting, both, non-attenuation-corrected and attenuation-corrected PET data is viewed as well as maximum intensity projections (MIP). The combination of a 40-row computed tomography with molecular high-resolution positron emission tomography ensures optimal image quality with improved spatial resolution up to 2 mm and a significant reduction of data acquisition time [41]. The HD PET-CT technology reduces image blurring tremendously. The integration of Time of Flight projections (TOF) in PET has further increased signal-to-noise ratio and improved small lesion detectability for micrometastases (see Figure 4). This is associated with shorter examination times and a reduction of FDG dose for the patient [41], [42], [43].

In 2000 the "evidence-based classification of the third Consensus Conference – Onko-PET III" discussed the indications for 18F-FDG PET-CT in HNSCC. According to the guidelines of the Consensus Conference it was decided to use PET-CT for staging of lymph nodes and distant metastases, the diagnosis of tumor recurrence in HNSCC, investigation of CUP and intensity modulated radiotherapy planning (IMRT) [44]. Whereas PET did not have the status of an essential diagnostic requirement in the "guidelines for tumors of the upper aerodigestive tract 2003" [45], to date there has been a paradigm shift. In the meantime, several studies admit the importance of 18F-FDG PET-CT for nodal staging of head and neck squamous cell carcinoma and the cervical CUP syndrome [37], [38], [39], [46], [47], [48]. 18F-FDG PET-CT can

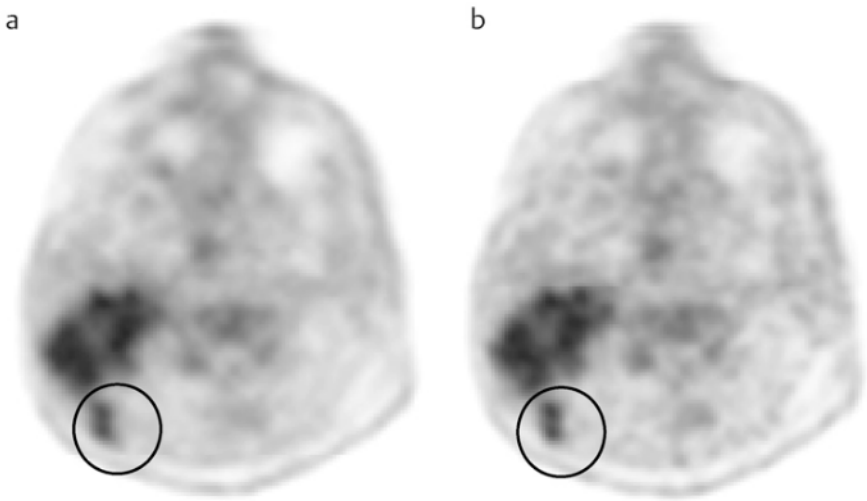

Figure 4: 53-year-old male with right sided cancer of the tonsil and histologically proven lymph node metastasis in the right neck level II (big lymph node) and two smaller lymph node metastases in level III (black circle). Standard reconstructions of the PET data with 3 iterations, 24 subsets, Gaussian filter 3 mm FWHM (Fig. 4a on the left side) and TOF reconstruction 3 mm with 3 iterations and 21 subsets (Fig. 4b on the right side). The 2 small lymph node metastases in the right neck level III appear with more sharply bounded outline and less blurring in the TOF reconstruction.

provide evidence of a second tumor during staging, considering the fact that in patients with HNSCC there is a 10 to 30-fold higher risk than in the general population for the development of secondary tumors outside the head and neck region. The incidence of secondary tumors in HNSCC patients ranges between 2.3% and 12% [49]. The presence of lymph node metastases in HNSCC has tremendous influence on the recurrence-free survival of the patients. With the detection of lymph node metastases, the 5-year survival rate decreases from initially about 50% to about 30% [37], [50]. 18F-FDG PET-CT is an established imaging modality for nodal staging in squamous cell carcinoma of the head and neck region. With a sensitivity of 87% to 90%, a specificity of 80% to 93% and a negative predictive value between 89% and 95%, 18F-FDG PET-CT can be used for the initial N-staging and for the detection of recurrent lymph node metastases [51]. While in the N0 neck no recommendation for a staging PET-CT exists and therefore N0 neck micrometastases remain a challenge, in the N1 neck 18 F-FDG PET-CT plays an important role in staging and downstaging of lymph nodes. Upstaging a N0 to a N1 neck or downstaging a N2b to a N2a neck involves adjustment or correction of the radiation field size and the surgical approach, which certainly contributes towards improved post-therapeutic quality of life for the patients [52].

The SUV value represents a prognostic marker in the treatment of HNSCC and is valuable for risk stratification in these patients [38], [39]. In the literature, SUV cut-off values between 1.9 to 3.0 are discussed for differentiation of benign from malignant lymph nodes [37], [38], [51]. Although the SUV can be influenced and affected by numerous physiological and technical factors, the threshold-based SUV quantification allows a differentiation between benign reactive lymph nodes from malignant lymph nodes with a sensitivity of 80% and a specificity of almost 99% [37], [53]. Lymph node metastases in HNSCC, diagnosed at an early stage, very often present with low SUV values which justifies a classification of these patients into a low risk group with good therapy response and corresponding recurrence free survival. Patients in the high risk group usually present with advanced tumor stages, high SUV values and limited therapy response [37], [38].

18 F-FDG PET-CT has a special status in the detection of the primary tumor in cancer of unknown primary (CUP). 5 to 10% of patients with CUP initially present with cervical lymph node swelling. The detection of the primary tumor can usually not be done successfully with inspection, palpation and endoscopy with biopsies alone. CT and MRI are mostly not sufficient for diagnosis. In suspected cervical HNSCC, 18 F-FDG PET-CT contributes towards primary tumor detection with a sensitivity of 75% to 88% and a specificity of 80% to 93%. However, 40% of CUP arise outside the head and neck region. In the literature, an initial CUP syndrome with successful diagnosis of the primary tumor is differentiated from a real CUP syndrome, where primary tumor detection is unsuccessful [54], [55], [56]. 3 to 5% of all malignancies become manifest as CUP syndrome. Histologically, approximately 80% of CUP are moderate to poorly differentiated adenocarcinomas, 5% are undifferentiated carcinomas and only about 10% are squamous cell carcinomas [54]. CUP syndrome, depending on the extent of disease, present with many different patterns of metastases. In case of infiltration of the jugular lymph nodes in the neck regions I and II [7], the primary tumor is often to be found in the tonsils, the base of the tongue, the nasopharynx or the piriform recess [37], [57]. In these cases a 5-year survival rate of about 63% is reported in the literature [54]. The detection of a primary tumor in the pharynx is a challenge due to the physiological FDG accumulation in the Waldeyer's ring. Are the caudal lymph nodes affected in the levels IV and V [7], the underlying cause is mainly hypopharynx

or bronchial cancer. 5-year survival rate decreases up to 10% when lymph node metastases in the caudal levels are affected [54].
In case of an initial cervical CUP syndrome, 5-year survival rate can increase up to 90%, considering that early stage tumor detection is achieved by 18F-FDG PET-CT. In real CUP syndrome FDG PET-CT may allow estimation of overall survival time, depending on tumor stage and extent of distant metastases, even if the primary tumor remains undetected [54]. Before the establishment of 18F-FDG PET-CT for the diagnosis of CUP syndrome, the treatment algorithm in suspected HNSCC included clinical examination, endoscopy and biopsy, bilateral tonsillectomy or partial resection of the base of the tongue as well as neck dissection, if needed [54], [55]. Currently invasive diagnostic procedures can be avoided. In cases of suspected squamous cell CUP syndrome, primary tumor detection can now be achieved with a sensitivity and specificity of over 80% with 18F-FDG PET-CT [37].

3.2 18 F Fluorodeoxyglucose PET-CT for therapy response evaluation and outcome prediction in head and neck cancer

High standard diagnostic imaging is a prerequisite for adequate follow-up of HNSCC. The most important task of post-therapeutic imaging is the early detection of treatment non-responders, where the treatment regime has to be adapted to the radio-and chemosensitivity of residual tumor or tumor recurrence. This will prevent initiation of treatment which is expensive and not efficient, causing side-effects though. Treatment options in HNSCC, like head and neck surgery and radiotherapy cause fibrotic tissue remodeling, scarring and post-radiation induced inflammation, rendering the distinction between still active tumor tissue and avital tumor necrosis difficult, even if morphological assessment demonstrates a reduction in tumor or lymph node size. This explains, why conventional follow-up with CT or MRI alone and the application of RECIST criteria are not sufficient to evaluate therapeutic response reliably [58], [59]. The functional information on tumor metabolism is essential for diagnosis, which can be achieved by the PET examination.
Considering the fact, that most of the tumor recurrences in HNSCC occur in the first 2 years after diagnosis and treatment, and at this stage, the risk of distant metastasis is high, 18F-FDG PET-CT plays a key role in the post-therapeutic follow-up [48], [60]. As an imaging modality which provides metabolic information and morphological characterization of tissue, it is very valuable not only for the detection and staging of tumor and lymph node metastases, but also for response evaluation. After all, at the end of a therapy it is less the size of primary tumor and lymph node metastases but rather the estimation of residual vital tumor tissue that has impact on further therapy decisions [60]. Changes in glucose uptake and the SUV in the course of a therapy are markers for response evaluation. This assumes that PET-CT is always performed under standardized conditions. This applies to the termination of the study and the patients with regard to the FDG dose which has to be administered, fasting as well as physical activity of the patients. To ensure a standardized interpretation of findings, reconstruction algorithms for PET raw data and SUV quantification should also be adjusted and standardized [60]. Selection of pre-determined SUV cut-off values for response assessment of lymph node metastases is an established parameter for prediction of overall prognosis and has already been described in several studies [37], [38], [48]. Treatment non-responders usually demonstrate higher SUV values than therapy responders, in who treatment response correlates with decrease of SUV values. The investigation of a pre-and post-therapeutic target volume seems to be less suitable for assessment of therapy response. For response assessment Chung et al. [61], [62] defined a pre-therapeutic “metabolic tumor volume” (MTV) of 40 ml in patients with carcinoma of the pharynx. Patients with a post-therapeutic MTV greater than 40 ml showed worse relapse-free survival rates than patients with an MTV below 40 ml. However, in this study post-radiation induced inflammation as a cause of increased tissue volume remained unconsidered, which can also affect the differentiation between tumor and non-tumorous tissue. For precise estimation of metabolic tumor response in PET, information on tumor cell proliferation, tumor oxygenation and tissue hypoxia is required and needs to be analyzed with appropriate molecular markers. Therefore specific tracers such as methionine, fluorothymidine or ethyltyrosine are used [63]. Only then, when tumor response to cytostatic treatment and its intrinsic radioresistance can be assessed, an outcome prediction in terms of treatment efficiency and relapse-free survival rate is possible. For hypoxia imaging in PET-CT dedicated hypoxia markers are available, which will be discussed in chapter 3.3 [63].
Many studies have confirmed the high predictive value of 18F-FDG PET-CT for response evaluation in HNSCC [37], [48], [64]. In Table 2 several clinical studies that analyse the role of 18F-FDG PET-CT for response evaluation and outcome prediction in patients with HNSCC are compared with eachother [64], [65], [66], [67], [68], [69]. The results, according to the review of the literature, show that the NPV for 18F-FDG PET-CT for the N0 neck but also in advanced tumor stages, ranges between 80% to 99%. Especially in the study by Malone et al. in 2009, therapy response following combined radio-chemotherapy for the primary tumor and neck lymph node metastases is analysed, with indication of the negative and positive predictive value of PET-CT for the N0 and the N1-N3 neck. In both groups 18 F-FDG PET-CT achieved a specificity of 90% with a NPV of 94% for the N1-3 neck and 92% for the N0 neck. Patients who did not present with increased SUV levels in the lymph nodes in PET-CT, were expected to have a better outcome than patients without post-therapeutic decrease in SUV values [67]. In cases where a post-therapeutic 18F-FDG uptake is observed, further

Table 2: Value of 18F-FDG PET-CT for response evaluation and outcome prediction in patients with HNSCC

Author	Year	Follow-up interval	Number patients	Response evaluation parameters	Outcome prediction results	Treatment	Notes
Brun et al. [65]	2002	5 years	47	SUV Median cut-off for: 1. Remission 2. Recurrence-free 3. Local tumor control	Low SUV 1. 96% (n=45) 2. 72% (n=34) 3. 96% (n=45) High SUV 1. 62% (n=29) 2. 35% (n=16) 3. 55% (n=26)	Radio-chemo-therapy	Advanced HNSCC
Andrade et al. [64]	2006	1 year + 5 months	28	1. Sensitivity recurrence detection 2. Specificity recurrence detection 3. Accuracy after 8 weeks for recurrence detection	1. 62% 2. 93% 3. 86%	Radiation	Correlation with histopathology
Connell et al. [66]	2007	2 years + 4 months	76	1. Change in TNM-classification 2. Influence on radiation planning 3. Metabolic response	1. 34% (n= 26) 2. 29% (n= 22) 3. 43% (n= 33)	Radio-chemo-therapy	—
Malone et al. [67]	2009	2 years	31	1. Sensitivity primary tumor/N0 neck/N1-3 neck 2. Specificity primary tumor/N0 neck/N1-3 neck 3. PPV primary tumor/N0 neck/N1-3 neck 4. NPV primary tumor/N0 neck/N1-3 neck	1. 83%/–/75% 2. 54% /92%/94% 3. 31%/ – />75% 4. 92%/93%/94%	Radio-chemo-therapy	Correlation with histopathology
Passero et al. [68]	2010	2 years	53	1. Clinical outcome 2. CT outcome 3. PET-CT outcome	1. 79% (n=42) 2. 51% (n=27) 3. 93% (n=50)	Radio-chemo-therapy	Advanced HNSCC

evaluation by biopsy or surgery is recommended. To avoid false positive findings in 18F-FDG PET-CT, the general recommendation is to proceed to investigations for response evaluation and outcome prediction not sooner than 8 to 12 weeks after completion of therapy. In case of earlier diagnostic work-up, the specificity of PET-CT is not sufficient to distinguish post-therapeutic edema or scarring from tumor recurrence or residual tumor [37], [64], [70]. The posttherapeutic care of patients with HNSCC using 18F-FDG PET-CT is justified, as it represents a surrogate marker for treatment success and local tumor control after radio-chemotherapy [63], [64]. Good therapy response ultimately correlates with a better quality of life due to optimized treatment with minimal side effects.

Increasing knowledge on specific biomolecular markers in head and neck squamous cell carcinoma which are responsible for tumor cell proliferation, angiogenesis, apoptosis and metastasis, promote the development of new treatment approaches. Individualized antiproliferative tumor therapies are targets for advanced HNSCC with lymph node metastases and focus on the blockade of Endothelial Growth Factor Receptor (EGFR) and Vascular Endothelial Growth Factor Receptor (VEGFR), both relevant for tumor cell progression and angioinvasion [69], [71]. Monoclonal antibodies such as cetuximab or tyrosine kinase inhibitors are responsible for local tumor cell growth control. They induce reduction of tissue hypoxia in the tumor and thus its intrinsic radioresistance can be increased to lower the mortality of patients with advanced HNSCC [60], [69], [71]. A successful cetuximab therapy blocks the extracellular domain of the EGF receptors, leading to local control of tumor growth and metastasis. High EGFR levels in the tissue, however, are often associated with radio-and chemotherapy resistance, requiring a conversion of anticancer therapy, as used in intensity-modulated radiotherapy (IMRT) and dose modulation in the treatment planning (see Chapter 3.3) [72], [73].

One of the main contributions of PET-CT, being a functional and metabolic imaging modality, lies in the noninvasive quantification of the therapeutic effect. Response evaluation and outcome prediction include both, the patient selection for targeted radio-chemotherapy as well as an efficient cost-benefit risk stratification for patients to ensure optimal individualized tumor therapy [72], [73].

3.3 Tumor hypoxia imaging: influence of non-FDG PET tracer on therapy planning in head and neck cancer

Hypoxia imaging of HNSCC is very decisive for planning the therapeutic approach. Dedicated hypoxia tracer enable determination of tumor and lymph node metastases oxygenation before and during treatment in order to assess their radio-and chemosensitivity [60], [73], [74]. Tumor cell hypoxia is based on a cascade of molecular processes that trigger cellular and metabolic changes in the tissue. These lead to an acute and chronic hypoperfusion but also hypooxygenation of tumor tissue, which causes a stimulation of tumor angiogenesis which might induce resistance to radio- and chemotherapy [72], [74], [75]. This results in induction of cell proliferation with increased aggressiveness of the tumor and metastatic potential [76], [77].

Since hypoxia represents a negative prognostic factor for tumor progression and resistance to treatment, hypoxia imaging, especially in advanced HNSCC, plays an important role for treatment monitoring and response evaluation [74], [78]. In the course of treatment, the degree of tumor oxygenation in HNSCC changes. The extent of hypoxia as a predictive factor, influences the survival time of patients [75]. PET-CT enables diagnosis of tumor hypoxia in the course of treatment and thus an optimization of chemotherapy and radiotherapy can be achieved [76]. In contrast to the method described in literature, where invasive measurement of hypoxia is performed by inserting Eppendorf electrodes in tumor tissue, PET enables non-invasive assessment of tumor perfusion and the hypoxia index with dedicated hypoxia tracers and therefore is less invasive for the patient [79], [80]. Also, immunohistochemical analysis of tissue after biopsy in order to differentiate between tumor and scar tissue are invasive and dependant on sufficient biopsy sampling sizes.

Sensitive PET tracers for hypoxia imaging in HNSCC are the presently available hypoxia markers 18 Fluoromisonidazol fluorine (18F-FMISO) and Fluorine-18 Fluoroazomycin arabinoside (18 F-FAZA) for assessment of therapeutic outcome of patients [60]. 18F-FMISO is a highly lipophilic tracer, which is predominantly eliminated via the hepato-biliary tract. Due to the pronounced lipophilicity, 18F-FMISO accumulates very gradually in hypoxic tissue and correspondingly is eliminated very slowly from healthy, non-hypoxic tissue [74], [76], [77]. Due to these pharmacokinetic properties of the tracer, the PET examination should not be initiated sooner than 90 to 140 minutes after injection. Nevertheless, image quality of PET images may still be limited by the reduced tumor-to-background contrast [73], [81]. In contrast to 18F-FDG PET-CT which is usually performed 1 hour after tracer application, hypoxia imaging requires good patient compliance throughout the examination.

18F-FAZA is characterized by a lower lipophilicity than 18F-FMISO, accumulates much faster in hypoxic tissues, and is characterised by exclusively renal elimination [73], [77]. Souvatzoglu et al. investigated the value of 18F-FAZA PET for radiation planning in patients with HNSCC and were able to demonstrate that hypoxic tumor tissue shows much more intensive tracer uptake than surrounding healthy muscle tissue. By determining the “tumor-to-muscle uptake ratio” and the SUV quantification between hypoxic and non hypoxic tissues, this tracer can be used for sequential quantitative assessment of tumor hypoxia before, during and after therapy [78]. In particular, dynamic PET studies with post-processing using pharmacokinetic models allow a better identification of hypoxic target volume [81].

Hypoxia imaging provides relevant information for treatment planning in HNSCC. It enables dose escalation in hypoxic tumor tissue while sparing non hypoxic surrounding tissue. This contributes to a reduction of post radiation side effects and consecutive improvement of the quality of life in these patients inspite of intensified radiation dose. Yet the main requirement of hypoxia imaging remains dose adjustment for intensity-modulated radiotherapy (IMRT). It also allows to select local treatment options that improve tumor oxygenation and thus improve radiosensitivity. These local treatment options include hyperbaric oxygen therapy and administration of erythropoietin and blood transfusions. Hypoxia imaging may also consider the need for tumor therapy with the cytostatic drug Tirapazamine. It selectively attacks hypoxic cells in tumor tissue, is metabolized in hypoxic tissue and produces free radicals under hypoxic conditions, which destroy tumor cell DNA [82].

Intensive review of the literature shows that 18F-FMISO and 18F-FAZA are the most frequently used PET tracer for hypoxia imaging in HNSCC and long-term experience with these tracer is available [73], [77], [78], [81]. The thymidine analogue 18F-fluoro-3-deoxy-3-L-fluorothymidine (18 FLT) is being used for PET examinations of cell proliferation in solid tumors such as sarcomas and GIST tumors, although it has not been established for PET imaging in HNSCC [73].

In some publications, the value of hypoxia imaging was compared with dynamic contrast-enhanced MRI (DCE-MRI) and investigated in several studies. In a study by Jansen et al. 13 patients underwent 18F-FMISO PET as well as DCE-MRI before and after radio-chemotherapy [83]. The investigation focused on the analysis of suspicious lymph nodes at initial diagnosis of HNSCC. Lymph nodes which were detected on DCE-MRI were first examined morphologically, followed by dynamic evaluation of their cell density and perfusion using compartment model analysis [84], [85]. The measured size of the lymph nodes detected on DCE-MRI correlated with the SUV of

the lymph nodes in PET-CT. However, there was a negative correlation between lymph node perfusion in MRI and oxygenation status in PET. Poorly perfused lymph nodes showed significantly elevated SUV values in PET, which led to a dose escalation during IMRT planning in ordert o improve therapeutic outcome [83].
Also Dirix et al. and Wang et al. emphasize the importance of 18F-FMISO hypoxia imaging for IMRT planning [75], [81]. In their studies they confirm that hypoxia is a negative prognostic marker for recurrence-free survival of patients with squamous cell carcinoma of the head and neck region and, consequently, individualized tumor therapy should be sought for eradication of hypoxia and improvement of treatment outcome. The prerequisite for optimal treatment planning is being fulfilled with the use of dedicated hypoxia markers for PET imaging in HNSCC.

4 Magnetic Resonance Imaging (MRI)

4.1 Impact of high-field MRI on the assessment of locoregional spread of head and neck cancer

For the exact evaluation of the tumour extent MRI requires an optimization of spatial resolution while maintaining adequate signal to noise ratio and minimizing scan time in order to avoid motion artefacts. This conflict between those 3 parameters with contradictory requirements can only be resolved by applying the most modern MR-techniques, ideally utilising high-field MRI systems with field strength of 3 Tesla, dedicated multi-element receiver coils and application of parallel acquisition techniques [86]. The latter method allows a substantial reduction of data acquisition by correction of the full high resolution data set with the coil sensitivity profiles of the signal receiver coil elements. In a recent study of Verduijn et al. [87], the technical requirements for optimal image quality in radiation treatment planning were defined as 0.4x0.4 mm slice thickness.
A high spatial resolution is also required for detailed assessment of the infiltration depth. In a retrospective study between 2003 and 2008 including 114 patients with HNSCC, Park et al found a significant correlation between the accurate detection of the infiltration depth on MRI and on histology [88]. The infiltration depth was significantly different between nodal positive and negative patients on T1-weighted sequences after contrast media with a cut-off for development of lymph node metastases of 9.5 mm for cancers of the oral tongue, yielding a sensitivity of 83% and a specificity of 68%, and 14.5 mm for cancers of the tongue base with a sensitivity of 79% and a specificity of 67%. With regard to the relevant structures defining resectability of tumours in the head and neck area, in particularly the arterial encasement, infiltration of the prevertebral fascia, of the mediastinum, trachea, oesophagus and larynx as well as the skull base, the mandibula and the brachia plexus, MRI overall demonstrates a higher sensitivity than CT exceeding 90% while specificity is lower reaching only 80 to 85% [25]. This is of particular importance for the first 3 criteria defining non resectable stage 4b carcinomas by the classification of the American Joint Commission on Cancer (AJCC). The preservation of the retropharyngeal fat plain on MRI was shown to have a negative predictive value of 97% with regard to exclusion of an infiltration of the prevertebral space [89].
In a recent study of Gu et al. [24], the synergistic use of combined MRI, CT and PET-CT revealed the highest accuracy for detecting infiltration of the mandibula. This added value of combined MRI and PET image assessment is also supported by several studies of software-assisted image fusion, particularly for planning of radiation therapy. On the one hand, MRI has advantages in the head and neck area compared to CT, due to lesser artefacts from dental implants as well as better delineation of tumours against the surrounding mucosa, submucosa, salivary glands and tongue base, on the other hand, PET is superior for the differentiation of vital tumour tissue versus inflammatory changes after radiation treatment. In a prospective study of 65 patients with head and neck tumours, the fusion of MR and PET images increased the sensitivity from 67 to 92% for assessment of recurrent disease with only little decrease of the positive predictive value to 95%, whereas for primary staging no significant advantage was found for image fusion compared to individual assessment of MR and PET data [90]. For MRI, the combination with integrated PET acquisition holds great potential in the future particular since functional assessment by dynamic contrast enhancement on MRI can be combined in real time with various PET tracers for further improvement of accuracy and more detailed insights into tumour biology. The first hybrid systems with a true combined MR and PET acquisition are commercially available since late 2011. In an initial feasibility study of 8 patients with head and neck tumours an excellent image quality without artefacts was found and the values for tumour metabolism assessed by the integrated PET component compared well to the preceding PET-CT study [91].

4.2 Modern MRI techniques for the assessment of dignity of cervical lymph nodes and therapeutic monitoring

The main limitation of radiological cross-sectional imaging, both CT as well as MRI, is the identification of malignant lymph nodes, which do not reach the morphologic size and shape criteria. For this reason, studies with a cut-off value of >1 cm size, respectively longitudinal to cross-sectional ratio of <2 for definition of a malignant lymph node only reach a sensitivity of 80% with a specificity of 60% [92]. Although De Bondt could demonstrate an additional diagnostic value by determining the signal intensity at the margin and in the center of the lymph node on

T2-weighted images as compared to the measurement of the cross-sectional diameters alone in lymph nodes >1 cm, this approach revealed only a moderate accuracy in lymph nodes with <1 cm in size [93]. Therefore, new methods have been developed within the last 10 years which besides morphological criteria also apply functional and metabolic parameters as well as the analysis of the microstructure and cellular composition.

4.2.1 MR-perfusion and MR-spectroscopy

For assessment of lymph node perfusion, mainly techniques of dynamic contrast enhancement (DCE) with standard extracellular Gadolinium chelates are applied for assessment of the temporal evolution of contrast media enhancement and calculation of semi-quantitative parameter maps. For determination of tumour metabolism in lymph nodes, MR-spectroscopy (MRS) is used deriving different frequency spectra which are representative for the different metabolism in normal and tumorous tissue. In a study of 39 patients, MRS found significantly different choline-to-creatine ratios of 22 malignant lymph nodes as compared to benign ones [94]. Both techniques of DCE and MRS have in common that the methods are complex and subject to artefacts on one hand and on the other hand could only moderately raise the accuracy for characterization of malignant lymph nodes [95]. Particularly the specificity of dynamic susceptibility weighted perfusion quantification (DSC) reached only 83% in a current study of 2011, although with a sensitivity of 97% [96]. Due to the limited spatial resolution of DSC-sequences respectively, the limited signal of MRS at field strengths of 1.5 Tesla the overall assessment of malignant lymph nodes is limited to a minimum size of 1 cm. This particularly limits the characterization of small lymph node metastases which have a major impact on the surgical approach.

4.2.2 New MR contrast agents

MR methods for assessment of the cellular composition and micro-structure of lymph nodes represent a different technical approach. MR contrast agents with uptake in the reticuloendothelial system (RES) by macrophages or histiocytes such as ultra-small particle iron oxides (USPIO) or elimination by the lymphatic system due to strong, reversible binding to large serum proteins allow the identification of metastatic lymph nodes through accumulation of malignant cells which results in reduction of their phagocytosis and reduced lymphatic transport. MRI with USPIO applies strongly T2*-weighted sequences for detection of local signal decay from the accumulation of the small iron particles. In case of strong signal decay, i.e. a black lymph node, a normal RES activity can be assumed. If there is no signal decay, i.e. the lymph node remains bright, metastatic infiltration is likely. The general advantage of this technique is the detection of even micrometastases in otherwise normal lymph nodes, as has been shown in studies of prostate cancer [97]. However, there is some overlap of the signal characteristics in reactively enlarged benign lymph nodes for example by their fatty core which does not take up USPIO either. Between 1995 and 2005, several studies have been performed for assessment of the value of this contrast agent, reaching only phase 3 of the clinical approval. In monocentric studies, the accuracy was substantially superior compared with the standard, morphology based MR criteria, whereas these positive results could not be fully confirmed in the multicentric studies substantially limiting the overall MR approval of these agents [98], [99], [100]. Strongly protein-binding substances reveal the opposite signal mechanism, i.e. benign lymph nodes appear bright compared to malignant ones due to the accumulation of protein-bound gadolinium chelates in lymph nodes resulting in T1 shortening. This mechanism is blocked in case of metastatic lymph node infiltration and lack of lymphatic clearance of the contrast agent [101]. For head and neck imaging, there are no data from systematic studies for this type of contrast agent as the substance Gadofosveset has been withdrawn from the market for strategic reasons shortly after approval in Europe. Nevertheless, initial studies in rectal cancer demonstrate promising results with high accuracy [102].

In a meta-analysis from 2007 the performance of MRI solely based on morphologic criteria as well as with the use of USPIO was systematically compared to CT, ultrasound and ultrasound-guided fine needle aspiration. On the basis of MEDLINE, EMBASE and Cochrane data base search between 1990 and 2006, a total of 17 articles with 25 data sets were analysed using the inclusion criteria of histology proven HNSCC and histopathologically confirmed lymph node metastases [92]. Overall standard MRI applying the criteria of morphology, signal intensity on T1- and T2-weighted sequences as well as uptake of standard extracellular contrast media was slightly inferior to CT with identical mean sensitivity of 81% but lower specificity of only 63% as compared to 76%. For both modalities, there was a remarkable heterogeneity of the size criteria for malignant lymph nodes with ranges between 10–15 mm for the longitudinal and 5–7 mm for the cross-sectional diameter, in part depending on the regional level of lymph node assessment. The 2 included studies with USPIO-enhanced MRI could raise the mean specificity substantially to 88% however on the expense of a lower sensitivity of only 74%. Solely the 3 studies of ultrasound-guided fine needle aspiration could demonstrate an acceptable sensitivity of 80% by maintaining a high specificity of 98%. Therefore, the authors concluded that the accuracy of MRI is currently not sufficient for lowering the a posteriori likelihood for occult lymph node metastases below 20% and therefore clinically defining an N0-stage since for the latter both a high sensitivity as well as an acceptable specificity is mandatory.

4.2.3 Diffusion-weighted imaging

Within the last 5 years diffusion-weighted imaging (DWI) has been applied outside the central nervous system as

Table 3: Overview of current literature for DWI MRI in HNSCC

Author	Journal	Year	n LN	Design	Reference	ADC cut-off [10^{-3}mm^2/s]	Sens [%]	Spec [%]	NPV [%]	PPV [%]
Holzapfel [138]	EJR	2009	55	p	H (n=33) F/U (n=17) PET (n=5)	1.02	100	87	100	90.9
Vande-caveye [33]	Radio-logy	2009	301		H	0.94	84	94	95	82
De Bondt [139]	AJNR	2009	219	p	H	1.0	92	84	99	44
Razek [140]	Eur Radiol	2006	87	p	H	1.38	98	88	84	99
Perrone [141]	Eur J Radiol	2006	32*	r	H, F/U	1.03	100	93		

*Patients. Abbreviations: LN = Lymph nodes, Sens = Sensitivity, Spec = Specificity, NPV = negative predictive value, PPV = positive predictive value, H = histopathology, F/U = follow-up, PET = positron emission tomography, ADC = apparent diffusion coefficient, p = prospective, r = retrospective

the classical area of implementation and currently demonstrates the most promising results with regard to detection of malignant lymph nodes. The underlying principal is based on the detection of the thermally induced Brownian molecular motion (BM) of water by switching of bipolar magnetic field gradients. In normal tissue BM is high particularly in the extra-vascular, extracellular space resulting in spin dephasing with consecutive signal decay. If the size of the extra-vascular, extracellular space is reduced such as in the case of cell swelling from hypoxia or densely packed tumour cell-lines, BM will be reduced with consecutive preservation of signal on DWI. However, diffusion can be restricted both in scar tissue as well as in benign lymph nodes; therefore, this phenomenon by itself does not suffice for differentiation between benign and malignant lymph nodes, but requires the calculation of the so called apparent diffusion coefficient (ADC). Hereby, multiple bipolar magnetic field gradients of different duration, frequency and amplitude (so called b-values) are used and typically a mono-exponential fit is applied to the signal decay. The ADC is expressed in 10^{-3} mm^2/s units and is a quantitative measure of the extent of diffusion restriction. However, this value is influenced by technique-related variations such as the choice of the different b-values, the degree of diffusion-weighting, the type of sequences (breath-hold, free-breathing or respiratory-triggered) as well as partially by the use of different field-strengths. Particularly first generation high field MRI systems at 3 Tesla with single channel radiofrequency (RF) excitation result in substantial regional fluctuations of the ADC value due to dielectric artefacts, which are significantly reduced with second generation systems using dual-channel radiofrequency excitation. Also, the type of post-processing influences the ADC value by using mono-exponential, bi- or multi-exponential fits. In addition to these technical limitations, no single common threshold exists in clinical routine for the ADC value for differentiation between benign and malignant tissue. A detailed overview of the important studies with the individual ADC cut-off values and the resulting accuracies hereof can be found in Table 3. In a current publication from 2010, Holzapfel et al. reported an accuracy of more than 90% for the differentiation between malignant versus benign lymph nodes using an ADC cut-off value of 1.06 10^{-3} mm^2/s units. The main limitation of this study was the inclusion of only lymph nodes exceeding a size of 1 cm. In the same year, the group of Vandecaveye et al. found a sensitivity of 84% with a specificity of 95% for all lymph nodes. Remarkably, lymph nodes with a size of <1 cm were explicitly included in this study due to their high relevance for the therapeutic approach. In this subgroup the authors found a sensitivity of 76% with a specificity of 94%. The same group could show that highly-perfused tumours can potentially reveal erroneously high ADC values particularly if many low b-values and a standard mono-exponential fit are used [103]. Therefore, the authors recommended the determination of the ADC value on the b-1000 image and a cut-off between tumour and normal tissue of 0.94–1.03 10^{-3} mm^2/s which has to be postoperatively increased to 1.3 10^{-3} mm^2/s due to oedematous changes [104], [105]. A promising refinement of the technique is the use of optimized diffusion-weighted sequences such as the intravoxel incoherent motion method with bi-exponential fit for separation of the ADC value into a diffusion fraction D and a perfusion fraction f. Hereby, perfusion related effects can be differentiated from the true change of the micro structure by tumour cell infiltration [106]. So far, no systematic data exist for lymph node metastases in head and neck cancers.

False positive findings can be caused by granulomatous diseases from cellular infiltration of lymph nodes, however, overall DWI MRI with ADC calculation demonstrates an impressively high negative predictive value for exclusion of lymph node metastases exceeding a size of 4 mm which is particularly important for the exclusion of contralateral lymph node metastases prior to surgery or for planning of the radiation field. In a current study by Dirix

Table 4: Relationship between original DW images and corresponding ADC-value

	Signal on original DW images	ADC-value
Tumour	↑	↓
Fluid / necrotic tumour	↓	↑
Scar tissue	↓	↓
T2 shine through	↑	↑

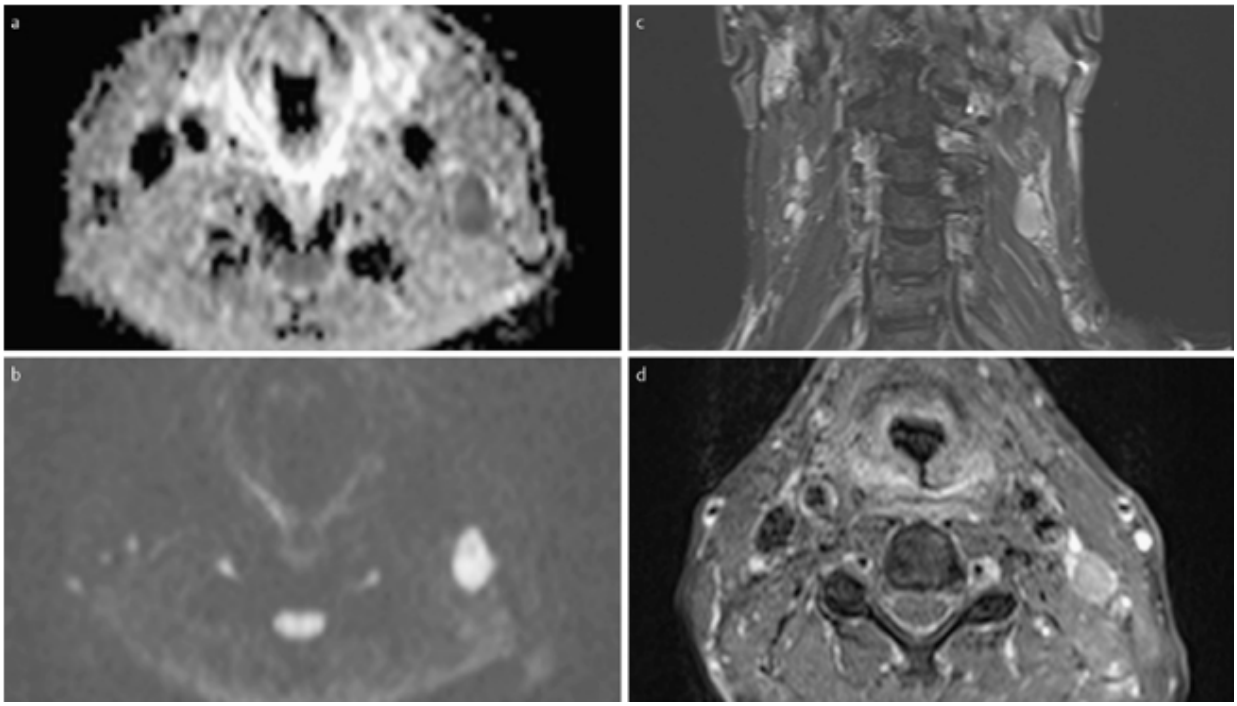

Figure 5: Lymph node metastasis in a patient with left-sided HNSCC of the oropharynx shows substantial diffusion restriction with signal increase in the axial original DW image (b) and corresponding decrease of the ADC value (a). Correlating display of the LN in the coronal fat-suppressed, fluid-sensitive STIR (c) and T1-weighted fat-suppressed image after contrast media (d).

et al. a high negative predictive value of DWI using a cut-off value of 0.94 10^{-3} mm^2/s was found with significant therapeutic impact due to better definition of the cross-target volume compared to conventional diagnostic work-up [107]. A limitation of the study is the retrospective data analysis from surgical cases. One advantage of DWI is the relatively low sensitivity towards inflammatory changes with preserved high specificity and high negative predictive value. In the future, this could result in a more elective use of neck dissection after radiochemotherapy with lowered morbidity. In fibrous scar tissue, the ADC can be as low as in tumour tissue, however, opposite to the latter there is a concomitant signal decrease in the original diffusion-weighted images which allows differentiation between both (Table 4). In lymph node metastases, there is usually a substantial diffusion restriction with signal increase in the original diffusion-weighted images with a consecutive decrease of the ADC value (compare Figure 5a–c). On the opposite, inflammatory tissue with high-fluid content can result in a massive signal increase in the original b0 DWI images with incomplete suppression of the signal even for high b-values analogous to tumour tissue (so called T2 shine through), however, the ADC value is increased which again allows the differentiation between inflammation and tumour. Problematic is the overlap between benign and malignant changes postoperatively in case of necrotic, partially liquified tumours with signal loss analogous to seromas in the original DWI images and a similar increase of the ADC value. The inclusion of a large amount (up to 48%) of this type of necrotic lymph nodes into the evaluation along with other specific acquisition parameters is assumed to account for the discrepant findings in the studies of Sumi et al. who found higher ADC values for malignant lymph nodes as for benign ones [108], [109].

4.2.4 Therapeutic monitoring

Several studies have shown that already the evaluation of tumours size on the basis of CT and preferentially MRI images allows for prediction of the course of the patient after treatment. A current study of Knegiens et al. in 360 patients with advanced HNSCC with a mean tumour volume of 37 cm^3 demonstrated the significant impact of tumour size on local tumour control and the overall survival after combined radiochemotherapy [110]. Using

Table 5: Prediction of therapeutic response

Publication	n	Parameter for prediction	Time points of DWI	ADC cut-off [10^{-3} mm^2/s] for response	Sens [%]	Spec [%]	PPV [%]	NPV [%]
Vandecaveye IJROBP 2012 [142]	29	2-year-loco-regional control	Baseline + 3 months	T: Δ ADC 25% LN: Δ ADC 20%			T: 89 LN: 70	T: 100 LN: 96
Berrak Acad Radiol 2011 [143]	18	Progression-free survival	Baseline + 3 months	LN: 22% ↑ ADC for Responders, 33% ↓ for Non-responders				
Kim Clin Canc Res 2009 [144]	33	Response at end of therapy	Baseline + 1 week after start of therapy + 2 weeks post treatment	LN: Baseline: ADC 1.11 after 1 week: 1.11 post treatment: 1.11	65 86 82	86 83 80		
Vandecaveye Eur Radiol 2010 [145]	30	2-year-loco-regional control	Baseline + 2 weeks after start of therapy + 4 weeks after start of therapy	T Δ ADC 14% LN Δ ADC 14,6% T Δ ADC 25% LN Δ ADC 19%	88 80 100 80	91 89 91 96	78 62 80 80	96 95 100 96
King Eur Radiol 2011 [146]	50	1-year-loco-regional control	Baseline + 2 weeks after start of therapy + 6 weeks post treatment for residual tumour	Non-responder: ADC ↓ during therapy ADC ≤ 1.4 post treatment	80 45	100 100	100	63

a cut-off value of 30 cm^3 the local 5-year-tumour control of smaller T3 tumours was 82% versus 55% of larger ones. Similar differences for local tumour control were also found for T4 tumours, whereas different TNM stages did not demonstrate a significant difference with regard to local tumour control. For overall survival only the n status had an additional influence. Therefore, the authors concluded that T stage should be subdivided into stage T3a or b, respectively, T4a or b depending on the tumour volume. In another current study, the determination of the tumour volume 6 weeks after completion of therapy revealed the highest predictive value for local therapy failure whereas additional volumetry 2 weeks after initiation of therapy did not have a significant impact. Therefore, volumetry alone does not allow for early modification of the therapeutic regimen, so far [111].

Meanwhile, several studies exist for assessment of therapeutic response based on DWI MRI allowing the prediction of both the therapeutic response after completion of therapy as well as the local regional control and progression free survival after 1, respectively 2 years with reasonable accuracy. Hereby, therapeutic response was found both for initially low b-values as well as for the increase of the ADC value 1 to 2 weeks after beginning of therapy. The change of the ADC value at the end of the therapy, respectively 3 to 6 weeks after therapy, compared to base line revealed the best predictive value for long-term locoregional tumour control (Table 5). A decrease of the ADC during therapy respectively the presence of large necrotic areas prior to therapy was associated with an adverse clinical course. Nevertheless, all publications conclude that for implementation of DWI into clinical routine multicenter studies are required for verification of these promising results. DCE-MRI also allows prediction of therapeutic response. In a study of Jansen et al. prediction of short-term, i.e. 3 to 4-month-long therapeutic response based on the parameter k_{trans} as a constant for contrast media redistribution was possible in comparison with PET as standard of reference [112]. Other studies from Kim et al. confirm the value of k_{trans} as a pre-therapeutic predictive marker for differentiation between patients with complete remission and

those with residual tumour after therapy. Hereby, patients with higher pre-therapeutic k_{trans} values revealed a significantly longer disease-free survival [113], [114].

4.3. Distant metastases

The frequency of distant metastases outside locoregional tumour spread ranges in the literature anywhere between 4 and 26% [115]. Besides pulmonary metastases which are a domain of PET-CT, mediastinal lymph nodes metastases are frequently found followed by liver and bony metastases. Particularly for the latter two, MRI using whole body acquisition with stepping table techniques has meanwhile developed as a time-efficient, cost-effective and accurate method. With increasing speed high-resolution protocols for local head and neck imaging can be integrated into the whole body acquisition with acceptable total scan times of 45 minutes. Already initial studies by Antoch et al. and Schmidt et al. found high accuracy for detection of distant metastases between 93 and 100% in non-selected patient clienteles with different tumour entities in comparison with PET-CT [116], [117], [118]. In a small prospective study of Herborn et al., the value of whole body MRI was specifically assessed for patients with HNSCC [115]. In this study, the TNM stage of all patients could be accurately determined by whole body MRI, however, in 4 patients with carcinoma of unknown primary the primary tumour could not be detected by any of the imaging methods. In a current study for detection of residual, respectively recurrent tumour in 179 patients with nasopharyngeal carcinoma (NPC) and presence of tumours in 31% whole body MRI revealed a sensitivity and specificity of 90%, both comparable with PET-CT [119]. Whole body MRI was superior to PET-CT for the assessment of intracranial tumour spread, retropharyngeal lymphadenopathy, necrotic lymph nodes and brain metastases. On the opposite, PET-CT was advantageous for the identification of vital tumour components in inflammatory tissue after radiation, lymph nodes metastases in normal size lymph nodes and pulmonary metastases. The combined analysis of whole body MRI and PET-CT allowed a further increase of sensitivity, for the assessment of local tumour spread both sensitivity and specificity could be raised.
In a current meta-analysis, the accuracy of whole body MRI exceeded that PET-CT for detection of bone metastases in breast cancer patients [120]. At the same time current data overall still shows inferiority of MRI for detection of lymph node metastases although current studies using diffusion-weighted MRI for whole body imaging demonstrate results comparable with PET-CT [121]. Further technical developments of this method using continuous table acquisition techniques allow further reduction of the total scan time to less than 30 minutes [122].

5 Head and neck surgery in head and neck squamous cell carcinoma

5.1 Demands made by the head and neck surgeon on multi-modality imaging

Radiological imaging has become an essential part in head and neck surgery. Along with the clinical findings as well as the results of panendoscopy, high-resolution imaging serves not only for the diagnosis of pathologies but also makes an increasingly important contribution to the treatment planning [123]. Especially in the head and neck region, it serves as a basis for determining the surgical procedure, the planning of the surgical approach, the assessment of the extent of the planned surgical intervention and the evaluation of potential risk factors which may occur during surgery. Essential preoperative information is obtained in particular by means of sectional imaging, namely by computed tomography (CT) and magnetic resonance imaging (MRI).
Owing to the extremely complex anatomy with narrow access and multiple relevant functional structures, head and neck surgery is generally considered to be very challenging [23], [124]. The head and neck region as such makes great demands on imaging, which, from the radiological point of view, necessitates a specialized knowledge in this field which is primarily obtained in an interactive communication between the head and neck surgeon and the radiologist [124].
However, it is of substantial importance that the clinician passes on precise information regarding clinical findings already obtained, implants utilized or local and distant flaps performed for reconstructive surgery [5], [124], [125]. By selecting the adequate imaging modality, the radiologist has to focus directly on the specific question of the surgeon as far as a tumour-induced vascular invasion, bony arrosion or lymph node metastasis is concerned. This not only ensures an accurate assessment of the pathological finding but also minimizes the burden and risk of other extensive and needless examinations for the patient [23], [125].
The main interest of the surgeon in head and neck oncology is focussed on the radiological assessment of the benign or malignant dignity of the tumour, the staging profile concerning local cervical lymph node metastases as well as distant metastases according to the TNM classification [5], [125]. Important evaluation criteria in terms of primary tumour, lymph node and distant metastases are tumour size and shape, depth of tumour extension and tumour infiltration of adjacent tissue structures. Special attention needs to be placed on the detection of high-risk tumour lesions, such as tumour-induced infiltration of the carotid sheath and the internal jugular vein or tumour-induced osteolysis [5], [125]. In particular inflammatory disorders as well as congenital and degenerative changes need to be ruled out as a possible differential diagnosis.

Paranasal sinuses and skull base

Regarding specific areas of the head and neck region, volume-rendered and computed tomography have proved to be the best imaging modality for the paranasal sinuses and the skull base.
According to the current guidelines of rhinosinusitis drawn up by the German Society of Oto-Rhino-Laryngology, Head and Neck Surgery (AWMF-Register No. 017/049; S2k guidelines, latest edition 03/2011), which also comprises malignant tumours in the nose and paranasal sinuses, computed tomography in axial sectioning with coronal reconstruction is considered to be the standard procedure [126], [127]. The consensus conference of the S2k Guidelines recommends a "low-dose" protocol for computed tomography in thin axial sectioning allowing multiplanar volume-rendered reconstructions [126], [128], [129]. To date, even volume-rendered reconstructed CT images provide full information for further necessary therapeutic steps [130]. Digital volume tomography for diagnostic purposes of the paranasal sinuses has recently become more and more popular. However, it is still too early to give a final statement in regard to its value compared to CT. Besides the assessment of the bony visceral cranium with distinction of the rhino- and otobasis, questions regarding an osseous destruction or infiltration of the dura, the apex of the orbit, the lamina papyracea and the pterygopalatine fossa are of essential importance [128], [131]. For better evaluation of soft tissue components and the anatomical relationship between neural and vascular structures, the application of a contrast agent is mandatory.
In advanced skull base tumours, a complementary MRI scan is needed to assess soft tissue tumours, a possible perineural tumour spread, as seen in adenoid cystic carcinoma, or an infiltration of the periorbit and the orbit itself [5], [125], [128].
As intraoperative navigation, which is nowadays regarded as a well-established standard in skull base and paranasal surgery, is based upon preoperative cross-sectional images, these interventions should not be performed without any CT images. The slice thickness of the CT images should be 1 mm to ensure a high-resolution reformatting during the navigation process, thus helping the surgeon with more confident orientation and surgical assistance [124], [125], [130], [132].

Nasopharynx

The evaluation of the nasopharynx is based not only on the clinical and endoscopic findings but also on the magnetic resonance imaging of soft tissue tumour structures. A major task of imaging has to be seen in the determination of the exact tumour extent and infiltration along the pharyngeal ring and the skull base. Very often nasopharyngeal carcinoma show a tumour extension into the pre-styloid compartment of the parapharyngeal region [5], [125]. Concomitant diseases, such as an effusion of the tympanic cavity, need to be diagnosed and interpreted correctly, as they can be an indirect sign of a tumour lesion. An intracranial tumour spread occurs either directly through a bony invasion of the skull base or through the sphenoid sinus and skull base foramina [5]. In cases of a suspected vascularized tumour in the nasopharynx, the tumour-feeding vessels need to be outlined by CTA or MRA. The main question then arising is whether the tumour vascularization originates from branches of the external carotid artery or the internal carotid artery and whether an embolization would be indicated.

Oral cavity and oropharynx

In more than fifty per cent, tumours of the oropharynx are primarily located in the tonsillar region [125]. Involving surrounding tissue structures, tonsillar tumours often infiltrate the soft palate, the base of the tongue, the lateral pharyngeal wall and medially the parapharyngeal space as well as the vascular sheath. Similarly, there may be an infiltration of the mandible. Osseous destruction of the mandible, especially located in the oral cavity region, can have a significant impact on the surgical treatment planning. It can influence immensely the extent to which plastic reconstructive measures need to be carried out after mandibulectomy [5], [124], [125]. Limitations of imaging, specifically of CT, are most commonly seen in the oral cavity region because of metal artefacts after dental restoration, which impair the evaluation of the examination with reduced value of information. As described in the literature it is not least for these reasons that MRI of the oral cavity and oropharynx is given preference over other imaging procedures, despite its lower specificity than CT.

Larynx and hypopharynx

In advanced-stage laryngeal malignancies the decisive question for the head and neck surgeon is whether the tumour infiltrates the cartilaginous framework of the larynx and shows signs of penetration into the parapharyngeal and pre-epiglottic space [26], [125]. As a main differential diagnosis it is necessary to rule out a chronic perichondritis of the cartilaginous laryngeal framework, as often seen after a concomitant radiochemotherapy. It is crucial to keep swallowing artefacts to a minimum during the imaging procedures. As described in literature, contrast-enhanced CT is recommended to determine the extent and spread of tumours of the glottis, while MRI is said to be the more valid method for laryngeal tumours of the supraglottis and the hypopharynx [5].

Cervical lymph nodes

A significant prognostic factor for squamous cell carcinoma of the head and neck region is the detection of cervical lymph node metastases. Similar to the T-classification for the primary tumour (T), cervical lymph nodes are classified according to the TNM classification (N) of

the UICC. Depending on the respective N-staging, further decisions are made in terms of surgical planning, the extent of radicality and prognosis [124], [125]. Helping to decide on these criteria, it is of crucial importance to determine to what extent the carotid sheath, especially the internal carotid artery, is tumour infiltrated or not. In cases of an infiltration, an additional carotid angiography with temporary occlusion of the internal carotid artery is mandatory to assess whether a resectability of the vessel is possible without any major complications. Another crucial aspect in deciding on a radical neck dissection procedure is the presence of an extracapsular tumour spread, which has a significantly worse prognostic factor [5], [124].

In recent years the introduction of PET-CT has revolutionized diagnostic measures in head and neck oncology. Especially in cases with a CUP syndrome (carcinoma of unknown primary), as well as in post-therapeutic oncological follow-up examinations PET-CT has proved to be an indispensable and well-established imaging tool to determine the N-stage in squamous cell carcinoma of the head and neck region. The same applies to the early detection of residual or recurrent tumours with PET-CT to evaluate the further prognostic status of the patient. Up to now there is still a lot of controversy whether a neck dissection is indicated in cases with a negative PET-CT finding for cervical lymph node metastases [5], [125].

5.2 Influence of imaging on the surgical treatment concept

For treatment planning, the head and neck surgeon can choose among a large variety of radiological and nuclear medicine imaging modalities. Imaging has experienced vast technological progress, becoming not only faster but also more accurate and providing the ability to detect even smaller lymph node metastases of only a few millimeters in size by PET-CT [123], [133], [134]. This is one of the reasons why a computer-aided planning of the operation is nowadays possible. The head and neck surgeon has to be able to transfer the generated CT and MRI data to his surgical site, which is certainly facilitated by the presence of multi-planar reconstructions [123], [134], [135]. The transfer of the imaging data to a haptic organ model, as it is already available for the paranasal sinus surgeries or with the IMOLA model (larynx model eligible for laser surgical intervention) for laryngeal surgeries, would enable a selective and intensified pre-operative training of the surgeon to improve his surgical skills [136], [137].

Abbreviations

ADC – Apparent Diffusion Coefficient
AJCC – American Joint Commission on Cancer
BM – Brownsche Molecular Movement
CT – Computed Tomography
CUP – Cancer of Unknown Primary
DCE – Dynamic Contrast Enhanced
DE-CT – Dual Energy CT
DSC – Dynamic susceptibility weightedPerfusion Quantification
DWI – Diffusion Weighted Imaging
EBV – Epstein Barr Virus
EGFR – Endothelial Growth Factor
FDG – Fluorodeoxyglucose
18F-FAZA – 18 F-Fluoroazomycin Arabinoside
18F-FDG – 18 F-Fluorodeoxyglucose
18F-FLT – 18 F-Fluoro-3-deoxy-3-L-Fluorothymidine
18F-FMISO – 18 F-Fluoromisonidazole
FWHM – Full Width Half Maximum
HD – High Definition
HNSCC – Head and Neck Squamous Cell Carcinoma
HPV – Human Papilloma Virus
IMOLA – Intervention applicable Laryngeal Model for Lasersurgery
IMRT – Intensity Modulated Radiotherapy
MD-CT – Multidetector-Computed Tomography
MIP – Maximum-Intensity-Projection
MRI – Magnetic Resonance Imaging
MRS – Magnetic Resonance-Spectroscopy
MRT – Magnetic Resonance Tomography
MTV – Metabolic Tumor Volume
NPC – Nasopharyngeal Carcinoma
NPV – Negative Predictive Value
PAT – Parallel Acquisition Techniques
PET-CT – Positron Emission Tomography-Computed Tomography
PPV – Positive Predictive Value
RECIST – Response Evaluation Criteria In Solid Tumors
RES – Reticulo-Endothelial-System
SUV – Standard Uptake Value
TOF – Time of Flight
USPIO – Ultra Small Particle Oxides
VEGFR – Vascular Endothelial Growth Factor Receptor

Notes

Competing interests

The authors declare that they have no competing interests.

References

1. Lell M, Hinkmann F, Gottwald F, Bautz W, Radkow T. Oropharynxpathologie [Oropharyngeal pathologies]. Radiologe. 2009 Jan;49(1):27-35. DOI: 10.1007/s00117-008-1763-1
2. Guntinas-Lichius O, Wendt T, Buentzel J, Esser D, Lochner P, Mueller A, Schultze-Mosgau S, Altendorf-Hofmann A. Head and neck cancer in Germany: a site-specific analysis of survival of the Thuringian cancer registration database. J Cancer Res Clin Oncol. 2010 Jan;136(1):55-63. DOI: 10.1007/s00432-009-0636-y
3. Castadot P, Lee JA, Geets X, Grégoire V. Adaptive radiotherapy of head and neck cancer. Semin Radiat Oncol. 2010 Apr;20(2):84-93. DOI: 10.1016/j.semradonc.2009.11.002

4. Hall SF, Groome PA, Irish J, O'Sullivan B. Radiotherapy or surgery for head and neck squamous cell cancer: establishing the baseline for hypopharyngeal carcinoma? Cancer. 2009 Dec 15;115(24):5711-22. DOI: 10.1002/cncr.24635

5. Vogl TJ, Mack MG, Gstöttner W. Kopf-Hals-Karzinom – Bildgebende Diagnostik. Onkologe. 2001;7:477-90. DOI: 10.1007/s007610170100

6. Tao Y, Daly-Schveitzer N, Lusinchi A, Bourhis J. Advances in radiotherapy of head and neck cancers. Curr Opin Oncol. 2010 May;22(3):194-9. DOI: 10.1097/CCO.0b013e3283388906

7. Werner JA. Lymphknotenerkrankungen im Kopf-Hals-Bereich. Berlin, Heidelberg, New York: Springer-Verlag; 2002. p. 3-42. DOI: 10.1007/978-3-642-55923-5_2

8. Fries R, Platz H, Wagner R, Stickler A, Grabner H, Kränzl B. Karzinome der Mundhöhle. Zur Frage der Abhängigkeit der Prognose von Alter und Geschlecht. Dtsch Z Mund Kiefer GesichtsChir. 1979;3:193-200.

9. Ragin CC, Modugno F, Gollin SM. The epidemiology and risk factors of head and neck cancer: a focus on human papillomavirus. J Dent Res. 2007 Feb;86(2):104-14. DOI: 10.1177/154405910708600202

10. Maier H, Fischer G, Sennewald E, Heller WD. Berufliche Risikofaktoren für Rachenkrebs. HNO. 1994;42:530-540.

11. Shao JY, Li YH, Gao HY, Wu QL, Cui NJ, Zhang L, Cheng G, Hu LF, Ernberg I, Zeng YX. Comparison of plasma Epstein-Barr virus (EBV) DNA levels and serum EBV immunoglobulin A/virus capsid antigen antibody titers in patients with nasopharyngeal carcinoma. Cancer. 2004 Mar;100(6):1162-70. DOI: 10.1002/cncr.20099

12. Ibrahim SO, Aarsaether N, Holsve MK, Kross KW, Heimdal JH, Aarstad JH, Liavaag PG, Elgindi OA, Johannessen AC, Lillehaug JR, Vasstrand EN. Gene expression profile in oral squamous cell carcinomas and matching normal oral mucosal tissues from black Africans and white Caucasians: the case of the Sudan vs. Norway. Oral Oncol. 2003 Jan;39(1):37-48. DOI: 10.1016/S1368-8375(02)00018-0

13. Shah SI, Yip L, Greenberg B, Califano JA, Chow J, Eisenberger CF, Lee DJ, Sewell DA, Reed AL, Lango M, Jen J, Koch WM, Sidransky D. Two distinct regions of loss on chromosome arm 4q in primary head and neck squamous cell carcinoma. Arch Otolaryngol Head Neck Surg. 2000 Sep;126(9):1073-6.

14. Wittekind C, Weber A, Weidenbach H. Pathologie und Prognosefaktoren von Plattenepithelkarzinomen des Kopf-Hals-Bereiches. Onkologe. 2001;7:498-504. DOI: 10.1007/s007610170102

15. Boehm A, Wichmann G, Mozet C, Dietz A. Aktuelle Therapieoptionen bei rezidivierenden Kopf-Hals-Tumoren. HNO. 2010;58:762-9. DOI: 10.1007/s00106-010-2156-0

16. Kawaguchi H, El-Naggar AK, Papadimitrakopoulou V, Ren H, Fan YH, Feng L, Lee JJ, Kim E, Hong WK, Lippman SM, Mao L. Podoplanin: a novel marker for oral cancer risk in patients with oral premalignancy. J Clin Oncol. 2008 Jan;26(3):354-60. DOI: 10.1200/JCO.2007.13.4072 DOI: 10.1200/JCO.2007.13.4072

17. Boonkitticharoen V, Kulapaditharom B, Leopairut J, Kraiphibul P, Larbcharoensub N, Cheewaruangroj W, Chintrakarn C, Pochanukul L. Vascular endothelial growth factor A and proliferation marker in prediction of lymph node metastasis in oral and pharyngeal squamous cell carcinoma. Arch Otolaryngol Head Neck Surg. 2008 Dec;134(12):1305-11. DOI: 10.1001/archotol.134.12.1305

18. Murakami R, Uozumi H, Hirai T, Nishimura R, Shiraishi S, Ota K, Murakami D, Tomiguchi S, Oya N, Katsuragawa S, Yamashita Y. Impact of FDG-PET/CT imaging on nodal staging for head-and-neck squamous cell carcinoma. Int J Radiat Oncol Biol Phys. 2007 Jun 1;68(2):377-82. DOI: 10.1016/j.ijrobp.2006.12.032

19. Yamazaki Y, Saitoh M, Notani K, Tei K, Totsuka Y, Takinami S, Kanegae K, Inubushi M, Tamaki N, Kitagawa Y. Assessment of cervical lymph node metastases using FDG-PET in patients with head and neck cancer. Ann Nucl Med. 2008 Apr;22(3):177-84. DOI: 10.1007/s12149-007-0097-9

20. Yamashina A, Tanimoto K, Sutthiprapaporn P, Hayakawa Y. The reliability of computed tomography (CT) values and dimensional measurements of the oropharyngeal region using cone beam CT: comparison with multidetector CT. Dentomaxillofac Radiol. 2008 Jul;37(5):245-51. DOI: 10.1259/dmfr/45926904

21. King AD. Multimodality imaging of head and neck cancer. Cancer Imaging. 2007;7 Spec No A:S37-46. DOI: 10.1102/1470-7330.2007.9013

22. Sham ME, Nishat S. Imaging modalities in head and neck cancer patients-overview. J Cancer Res Exp Oncol. 2011;3:22-5.

23. Aschenbach R, Esser D. Aktuelle Aspekte der posttherapeutischen Bildgebung bei Kopf-Hals-Malignomen [Post-therapeutic imaging strategies and follow-up in head and neck malignant tumours]. HNO. 2010 Aug;58(8):749-55. DOI: 10.1007/s00106-010-2143-5

24. Gu DH, Yoon DY, Park CH, Chang SK, Lim KJ, Seo YL, Yun EJ, Choi CS, Bae SH. CT, MR, (18)F-FDG PET/CT, and their combined use for the assessment of mandibular invasion by squamous cell carcinomas of the oral cavity. Acta Radiol. 2010 Dec;51(10):1111-9. DOI: 10.3109/02841851.2010.520027

25. Yousem DM, Gad K, Tufano RP. Resectability issues with head and neck cancer. AJNR Am J Neuroradiol. 2006 Nov-Dec;27(10):2024-36.

26. Becker M, Burkhardt K, Allal AS, Dulguerov P, Ratib O, Becker CD. Prä- und posttherapeutische Larynxbildgebung [Pretherapeutic and posttherapeutic laryngeal imaging]. Radiologe. 2009 Jan;49(1):43-58. DOI: 10.1007/s00117-008-1765-z

27. Li B, Bobinski M, Gandour-Edwards R, Farwell DG, Chen AM. Overstaging of cartilage invasion by multidetector CT scan for laryngeal cancer and ist potential effect on the use of organ preservation with chemoradiation. Br J Radiol. 2011 Jan;84(997):64-9. DOI: 10.1259/bjr/66700901

28. Becker M, Zbären P, Delavelle J, Kurt AM, Egger C, Rüfenacht DA, Terrier F. Neoplastic invasion of the laryngeal cartilage: reassessment of criteria for diagnosis at CT. Radiology. 1997 May;203(2):521-32.

29. Faggioni L, Neri E, Cerri F, Picano E, Seccia V, Muscatello L, Franceschini SS, Bartolozzi C. 64-row MDCT perfusion of head and neck squamous cell carcinoma: technical feasibility and quantitative analysis of perfusion parameters. Eur Radiol. 2011 Jan;21(1):113-21. DOI: 10.1007/s00330-010-1898-0

30. Kau RJ, Alexiou C, Laubenbacher C, Werner M, Schwaiger M, Arnold W. Lymph node detection of head and neck squamous cell carcinomas by positron emission tomography with fluorodeoxyglucose F 18 in a routine clinical setting. Arch Otolaryngol Head Neck Surg. 1999;125:1322-8.

31. Di Martino E, Nowak B, Hassan HA, Hausmann R, Adam G, Buell U, Westhofen M. Diagnosis and staging of head and neck cancer: a comparison of modern imaging modalities (positron emission tomography, computed tomography, color-coded duplex sonography) with panendoscopic and histopathologic findings. Arch Otolaryngol Head Neck Surg. 2000 Dec;126(12):1457-61.

32. Schroeder U, Dietlein M, Wittekindt C, Ortmann M, Stuetzer H, Vent J, Jungehuelsing M, Krug B. Is there a need for positron emission tomography imaging to stage the N0 neck in T1-T2 squamous cell carcinoma of the oral cavity or oropharynx?. Ann Otol Rhinol Laryngol. 2008 Nov;117(11):854-63.

33. Vandecaveye V, De Keyzer F, Vander Poorten V, Dirix P, Verbeken E, Nuyts S, Hermans R. Head and neck squamous cell carcinoma: value of diffusion-weighted MR imaging for nodal staging. Radiology. 2009 Apr;251(1):134-46. DOI: 10.1148/radiol.2511080128

34. Yoon DY, Hwang HS, Chang SK, Rho YS, Ahn HY, Kim JH, Lee IJ. CT, MR, US,18F-FDG PET/CT, and their combined use for the assessment of cervical lymph node metastases in squamous cell carcinoma of the head and neck. Eur Radiol. 2009 Mar;19(3):634-42. DOI: 10.1007/s00330-008-1192-6

35. Schmid-Bindert G, Henzler T, Chu TQ, Meyer M, Nance JW Jr,Schoepf UJ, Dinter DJ, Apfaltrer P, Krissak R, Manegold C, Schoenberg SO, Fink C. Functional imaging of lung cancer using dual energy CT: how does iodine related attenuation correlate with standardized uptake value of 18FDG-PET-CT? Eur Radiol. 2012 Jan;22(1):93-103. DOI: 10.1007/s00330-011-2230-3

36. Lell M, Baum U, Koester M, Nömayr A, Greess H, Lenz M, Bautz W. Morphologische und funktionelle Diagnostik der Kopf-Hals-Region mit Mehrzeilen-Spiral-CT. Radiologe. 1999;39:932-8. DOI: 10.1007/s001170050584

37. Subramaniam RM, Truong M, Peller P, Sakai O, Mercier G. Fluorodeoxyglucose-positron-emission tomography imaging of head and neck squamous cell cancer. AJNR Am J Neuroradiol. 2010 Apr;31(4):598-604. DOI: 10.3174/ajnr.A1760

38. Haerle SK, Strobel K, Ahmad N, Soltermann A, Schmid DT, Stoeckli SJ. Contrast-enhanced 18F-FDG-PET/CT for the assessment of necrotic lymph node metastases. Head Neck. 2011 Mar;33(3):324-9. DOI: 10.1002/hed.21447

39. Higgins KA, Hoang JK, Roach MC, Chino J, Yoo DS, Turkington TG, Brizel DM. Analysis of pretreatment FDG-PET SUV parameters in head-and-neck cancer: tumor SUVmean has superior prognostic value. Int J Radiat Oncol Biol Phys. 2012 Feb 1;82(2):548-53. DOI: 10.1016/j.ijrobp.2010.11.050

40. Liao CT, Wang HM, Huang SF, Chen IH, Kang CJ, Lin CY, Fan KH, Ng SH, Hsueh C, Lee LY, Lin CH, Yen TC. PET and PET/CT of the neck lymph nodes improves risk prediction in patients with squamous cell carcinoma of the oral cavity. J Nucl Med. 2011 Feb;52(2):180-7. DOI: 10.2967/jnumed.110.082370

41. Siemens Deutschland. Biograph mCT. http://www.siemens.de/MI

42. Kadrmas DJ, Casey ME, Conti M, Jakoby BW, Lois C, Townsend DW. Impact of time-of-flight on PET tumor detection. J Nucl Med. 2009 Aug;50(8):1315-23. DOI: 10.2967/jnumed.109.063016

43. Lois C, Jakoby BW, Long MJ, Hubner KF, Barker DW, Casey ME, Conti M, Panin VY, Kadrmas DJ, Townsend DW. An assessment of the impact of incorporating time-of-flight information into clinical PET/CT imaging. J Nucl Med. 2010 Feb;51(2):237-45. DOI: 10.2967/jnumed.109.068098

44. Reske SN, Kotzerke J. FDG-PET for clinical use. Results of the 3rd German Interdisciplinary Consensus Conference, "Onko-PET III", 21 July and 19 September 2000. Eur J Nucl Med. 2001 Nov;28(11):1707-23. DOI: 10.1007/s002590100626

45. Deutsche Gesellschaft für Hals-Nasen-Ohren-Heilkunde, Kopf- und Hals-Chirurgie e. V., Bonn [homepage on the Internet]. Available from: http://www.hno.org

46. Rödel R, Straehler-Pohl HJ, Palmedo H, Reichmann K, Jaeger U, Reinhardt MJ, Biersack HJ. PET-CT-Bildgebung bei Kopf-Hals-Tumoren [PET/CT imaging in head and neck tumors]. Radiologe. 2004 Nov;44(11):1055-9. DOI: 10.1007/s00117-004-1125-6

47. Fletcher JW, Djulbegovic B, Soares HP, Siegel BA, Lowe VJ, Lyman GH, Coleman RE, Wahl R, Paschold JC, Avril N, Einhorn LH, Suh WW, Samson D, Delbeke D, Gorman M, Shields AF. Recommendations on the use of 18F-FDG PET in oncology. J Nucl Med. 2008 Mar;49(3):480-508. DOI: 10.2967/jnumed.107.047787

48. Hustinx R, Lucignani G. PET/CT in head and neck cancer: an update. Eur J Nucl Med Mol Imaging. 2010 Mar;37(3):645-51. DOI: 10.1007/s00259-009-1365-9

49. Ng SH, Chan SC, Liao CT, Chang JT, Ko SF, Wang HM, Chin SC, Lin CY, Huang SF, Yen TC. Distant metastases and synchronous second primary tumors in patients with newly diagnosed oropharyngeal and hypopharyngeal carcinomas: evaluation of (18)F-FDG PET and extended-field multi-detector row CT. Neuroradiology. 2008 Nov;50(11):969-79. DOI: 10.1007/s00234-008-0426-2

50. Snow GB, Annyas AA, van Slooten EA, Bartelink H, Hart AA. Prognostic factors of neck node metastasis. Clin Otolaryngol Allied Sci. 1982 Jun;7(3):185-92. DOI: 10.1111/j.1365-2273.1982.tb01581.x

51. Richard C, Prevot N, Timoshenko AP, Dumollard JM, Dubois F, Martin C, Prades JM. Preoperative combined 18-fluorodeoxyglucose positron emission tomography and computed tomography imaging in head and neck cancer: does it really improve initial N staging? Acta Otolaryngol. 2010 Dec;130(12):1421-4. DOI: 10.3109/00016489.2010.502183

52. Lonneux M, Hamoir M, Reychler H, Maingon P, Duvillard C, Calais G, Bridji B, Digue L, Toubeau M, Grégoire V. Positron emission tomography with [18F]fluorodeoxyglucose improves staging and patient management in patients with head and neck squamous cell carcinoma: a multicenter prospective study. J Clin Oncol. 2010 Mar;28(7):1190-5. DOI: 10.1200/JCO.2009.24.6298

53. Sadick M, Kayed H, Pinol R, Frey S, Fink C, Schoenberg S, Brade J, Sadick H, Hoermann K, He V. "Challenges in Head and Neck Cancer": Optimisation of reconstruction algorithms in Truepoint HD PET/CT for improved diagnostic accuracy of lymph node metastases in head and neck squamous cell carcinoma. ECR-European Congress of Radiology; 03/2011; Vienna; Session 408.

54. Mozet C, Wuttke P, Bertolini J, Horn LC, Dietz A. Zervikale und axillare Metastasen unbekannten Ursprungs als CUP-Syndrom. Onkologe. 2008;14:898-907. DOI: 10.1007/s00761-008-1408-z

55. Bohuslavizki KH, Klutmann S, Kröger S, Sonnemann U, Buchert R, Werner JA, Mester J, Clausen M. FDG PET detection of unknown primary tumors. J Nucl Med. 2000 May;41(5):816-22.

56. Braams JW, Pruim J, Kole AC, Nikkels PG, Vaalburg W, Vermey A, Roodenburg JL. Detection of unknown primary head and neck tumors by positron emission tomography. Int J Oral Maxillofac Surg. 1997 Apr;26(2):112-5. DOI: 10.1016/S0901-5027(05)80829-X

57. Jenicke L, Bohuslavizki KH, Sonnemann U, Thoms J, Buchert R, Werner JA, Clausen M. FDG-PET in der Bildgebung des CUP-Syndroms. Onkologe. 2001;7:491-7. DOI: 10.1007/s007610170101

58. Yaghmai V, Miller FH, Rezai P, Benson AB 3rd, Salem R. Response to treatment series: part 2, tumor response assessment--using new and conventional criteria. AJR Am J Roentgenol. 2011 Jul;197(1):18-27. DOI: 10.2214/AJR.11.6581

59. Levine ZH, Galloway BR, Peskin AP, Heussel CP, Chen JJ. Tumor volume measurement errors of RECIST studied with ellipsoids. Med Phys. 2011 May;38(5):2552-7. DOI: 10.1118/1.3577602

60. Herrmann K, Krause BJ, Bundschuh RA, Dechow T, Schwaiger M. Monitoring response to therapeutic interventions in patients with cancer. Semin Nucl Med. 2009 May;39(3):210-32. DOI: 10.1053/j.semnuclmed.2008.12.001

61. Chung MK, Jeong HS, Park SG, Jang JY, Son YI, Choi JY, Hyun SH, Park K, Ahn MJ, Ahn YC, Kim HJ, Ko YH, Baek CH. Metabolic tumor volume of [18F]-fluorodeoxyglucose positron emission tomography/computed tomography predicts short-term outcome to radiotherapy with or without chemotherapy in pharyngeal cancer. Clin Cancer Res. 2009 Sep;15(18):5861-8. DOI: 10.1158/1078-0432.CCR-08-3290

62. Chung MK, Jeong HS, Son YI, So YK, Park GY, Choi JY, Hyun SH, Kim HJ, Ko YH, Baek CH. Metabolic tumor volumes by [18F]-fluorodeoxyglucose PET/CT correlate with occult metastasis in oral squamous cell carcinoma of the tongue. Ann Surg Oncol. 2009 Nov;16(11):3111-7. DOI: 10.1245/s10434-009-0621-3

63. Bussink J, van Herpen CM, Kaanders JH, Oyen WJ. PET-CT for response assessment and treatment adaptation in head and neck cancer. Lancet Oncol. 2010 Jul;11(7):661-9. DOI: 10.1016/S1470-2045(09)70353-5

64. Andrade RS, Heron DE, Degirmenci B, Filho PA, Branstetter BF, Seethala RR, Ferris RL, Avril N. Posttreatment assessment of response using FDG-PET/CT for patients treated with definitive radiation therapy for head and neck cancers. Int J Radiat Oncol Biol Phys. 2006 Aug 1;65(5):1315-22. DOI: 10.1016/j.ijrobp.2006.03.015

65. Brun E, Kjellén E, Tennvall J, Ohlsson T, Sandell A, Perfekt R, Perfekt R, Wennerberg J, Strand SE. FDG PET studies during treatment: prediction of therapy outcome in head and neck squamous cell carcinoma. Head Neck. 2002 Feb;24(2):127-35. DOI: 10.1002/hed.10037

66. Connell CA, Corry J, Milner AD, Hogg A, Hicks RJ, Rischin D, Peters LJ. Clinical impact of, and prognostic stratification by, F-18 FDG PET/CT in head and neck mucosal squamous cell carcinoma. Head Neck. 2007 Nov;29(11):986-95. DOI: 10.1002/hed.20629

67. Malone JP, Gerberi MA, Vasireddy S, Hughes LF, Rao K, Shevlin B, Kuhn M, Collette D, Tennenhouse J, Robbins KT. Early prediction of response to chemoradiotherapy for head and neck cancer: reliability of restaging with combined positron emission tomography and computed tomography. Arch Otolaryngol Head Neck Surg. 2009 Nov;135(11):1119-25. DOI: 10.1001/archoto.2009.152

68. Passero VA, Branstetter BF, Shuai Y, Heron DE, Gibson MK, Lai SY, Kim SW, Grandis JR, Ferris RL, Johnson JT, Argiris A. Response assessment by combined PET-CT scan versus CT scan alone using RECIST in patients with locally advanced head and neck cancer treated with chemoradiotherapy. Ann Oncol. 2010 Nov;21(11):2278-83. DOI: 10.1093/annonc/mdq226

69. Bonner JA, Harari PM, Giralt J, Cohen RB, Jones CU, Sur RK, Raben D, Baselga J, Spencer SA, Zhu J, Youssoufian H, Rowinsky EK, Ang KK. Radiotherapy plus cetuximab for locoregionally advanced head and neck cancer: 5-year survival data from a phase 3 randomised trial, and relation between cetuximab-induced rash and survival. Lancet Oncol. 2010 Jan;11(1):21-8. DOI: 10.1016/S1470-2045(09)70311-0

70. Horiuchi C, Taguchi T, Yoshida T, Nishimura G, Kawakami M, Tanigaki Y, Matsuda H, Mikami Y, Oka T, Inoue T, Tsukuda M. Early assessment of clinical response to concurrent chemoradiotherapy in head and neck carcinoma using fluoro-2-deoxy-d-glucose positron emission tomography. Auris Nasus Larynx. 2008 Mar;35(1):103-8. DOI: 10.1016/j.anl.2007.05.003

71. Bonner JA, Harari PM, Giralt J, Azarnia N, Shin DM, Cohen RB, Jones CU, Sur R, Raben D, Jassem J, Ove R, Kies MS, Baselga J, Youssoufian H, Amellal N, Rowinsky EK, Ang KK.Radiotherapy plus cetuximab for squamous-cell carcinoma of the head and neck. N Engl J Med. 2006 Feb;354(6):567-78. DOI: 10.1056/NEJMoa053422

72. Liu N, Li M, Li X, Meng X, Yang G, Zhao S, Yang Y, Ma L, Fu Z, Yu J. PET-based biodistribution and radiation dosimetry of epidermal growth factor receptor-selective tracer 11C-PD153035 in humans. J Nucl Med. 2009 Feb;50(2):303-8. DOI: 10.2967/jnumed.108.056556

73. Heuveling DA, de Bree R, van Dongen GA. The potential role of non-FDG-PET in the management of head and neck cancer. Oral Oncol. 2011 Jan;47(1):2-7. DOI: 10.1016/j.oraloncology.2010.10.008

74. Troost EG, Schinagl DA, Bussink J, Oyen WJ, Kaanders JH. Clinical evidence on PET-CT for radiation therapy planning in head and neck tumours. Radiother Oncol. 2010 Sep;96(3):328-34. DOI: 10.1016/j.radonc.2010.07.017

75. Dirix P, Vandecaveye V, De Keyzer F, Stroobants S, Hermans R, Nuyts S. Dose painting in radiotherapy for head and neck squamous cell carcinoma: value of repeated functional imaging with (18)F-FDG PET, (18)F-fluoromisonidazole PET, diffusion-weighted MRI, and dynamic contrast-enhanced MRI. J Nucl Med. 2009 Jul;50(7):1020-7. DOI: 10.2967/jnumed.109.062638

76. Troost EG, Schinagl DA, Bussink J, Boerman OC, van der Kogel AJ, Oyen WJ, Kaanders JH. Innovations in radiotherapy planning of head and neck cancers: role of PET. J Nucl Med. 2010 Jan;51(1):66-76. DOI: 10.2967/jnumed.108.061499

77. Postema EJ, McEwan AJ, Riauka TA, Kumar P, Richmond DA, Abrams DN, Wiebe LI. Initial results of hypoxia imaging using 1-alpha-D: -(5-deoxy-5-[18F]-fluoroarabinofuranosyl)-2-nitroimidazole (18F-FAZA). Eur J Nucl Med Mol Imaging. 2009 Oct;36(10):1565-73. DOI: 10.1007/s00259-009-1154-5

78. Souvatzoglou M, Grosu AL, Röper B, Krause BJ, Beck R, Reischl G, Picchio M, Machulla HJ, Wester HJ, Piert M. Tumour hypoxia imaging with [18F]FAZA PET in head and neck cancer patients: a pilot study. Eur J Nucl Med Mol Imaging. 2007 Oct;34(10):1566-75. DOI: 10.1007/s00259-007-0424-3

79. Molls M, Feldmann HJ, Füller J. Oxygenation of locally advanced recurrent rectal cancer, soft tissue sarcoma and breast cancer. Adv Exp Med Biol. 1994;345:459-63. DOI: 10.1007/978-1-4615-2468-7_61

80. Bentzen L, Keiding S, Nordsmark M, Falborg L, Hansen SB, Keller J, Nielsen OS, Overgaard J. Tumour oxygenation assessed by 18F-fluoromisonidazole PET and polarographic needle electrodes in human soft tissue tumours. Radiother Oncol. 2003 Jun;67(3):339-44. DOI: 10.1016/S0167-8140(03)00081-1

81. Wang W, Lee NY, Georgi JC, Narayanan M, Guillem J, Schöder H, Humm JL. Pharmacokinetic analysis of hypoxia (18)F-fluoromisonidazole dynamic PET in head and neck cancer. J Nucl Med. 2010 Jan;51(1):37-45. DOI: 10.2967/jnumed.109.067009

82. Lee NY, Mechalakos JG, Nehmeh S, Lin Z, Squire OD, Cai S, Chan K, Zanzonico PB, Greco C, Ling CC, Humm JL, Schöder H. Fluorine-18-labeled fluoromisonidazole positron emission and computed tomography-guided intensity-modulated radiotherapy for head and neck cancer: a feasibility study. Int J Radiat Oncol Biol Phys. 2008 Jan;70(1):2-13. DOI: 10.1016/j.ijrobp.2007.06.039

83. Jansen JF, Schöder H, Lee NY, Wang Y, Pfister DG, Fury MG, Stambuk HE, Humm JL, Koutcher JA, Shukla-Dave A. Noninvasive assessment of tumor microenvironment using dynamic contrast-enhanced magnetic resonance imaging and 18F-fluoromisonidazole positron emission tomography imaging in neck nodal metastases. Int J Radiat Oncol Biol Phys. 2010 Aug;77(5):1403-10. DOI: 10.1016/j.ijrobp.2009.07.009

84. Lee FK, King AD, Ma BB, Yeung DK. Dynamic contrast enhancement magnetic resonance imaging (DCE-MRI) for differential diagnosis in head and neck cancers. Eur J Radiol. 2012 Apr;81(4):784-8. DOI: 10.1016/j.ejrad.2011.01.089

85. Chikui T, Kawano S, Kawazu T, Hatakenaka M, Koga S, Ohga M, Matsuo Y, Sunami S, Sugiura T, Shioyama Y, Obara M, Yoshiura K. Prediction and monitoring of the response to chemoradiotherapy in oral squamous cell carcinomas using a pharmacokinetic analysis based on the dynamic contrast-enhanced MR imaging findings. Eur Radiol. 2011 Aug;21(8):1699-708. DOI: 10.1007/s00330-011-2102-x

86. Casselman JW. High-resolution imaging of the skull base and larynx. In: Schoenberg SO, Dietrich O, Reiser MF, eds. Parallel imaging in clinical MR applications. Springer; 2007. p. 199-208. DOI: 10.1007/978-3-540-68879-2_19

87. Verduijn GM, Bartels LW, Raaijmakers CP, Terhaard CH, Pameijer FA, van den Berg CA. Magnetic resonance imaging protocol optimization for delineation of gross tumor volume in hypopharyngeal and laryngeal tumors. Int J Radiat Oncol Biol Phys. 2009 Jun 1;74(2):630-6. DOI: 10.1016/j.ijrobp.2009.01.014

88. Park JO, Jung SL, Joo YH, Jung CK, Cho KJ, Kim MS. Diagnostic accuracy of magnetic resonance imaging (MRI) in the assessment of tumor invasion depth in oral/oropharyngeal cancer. Oral Oncol. 2011 May;47(5):381-6. DOI: 10.1016/j.oraloncology.2011.03.012

89. Hsu WC, Loevner LA, Karpati R, Ahmed T, Mong A, Battineni ML, Yousem DM, Montone KT, Weinstein GS, Weber RS, Chalian AA. Accuracy of magnetic resonance imaging in predicting absence of fixation of head and neck cancer to the prevertebral space. Head Neck. 2005 Feb;27(2):95-100. DOI: 10.1002/hed.20128

90. Nakamoto Y, Tamai K, Saga T, Higashi T, Hara T, Suga T, Koyama T, Togashi K. Clinical value of image fusion from MR and PET in patients with head and neck cancer. Mol Imaging Biol. 2009 Jan-Feb;11(1):46-53. DOI: 10.1007/s11307-008-0168-x

91. Boss A, Stegger L, Bisdas S, Kolb A, Schwenzer N, Pfister M, Claussen CD, Pichler BJ, Pfannenberg C. Feasibility of simultaneous PET/MR imaging in the head and upper neck area. Eur Radiol. 2011 Jul;21(7):1439-46. DOI: 10.1007/s00330-011-2072-z

92. de Bondt RB, Nelemans PJ, Hofman PA, Casselman JW, Kremer B, van Engelshoven JM, Beets-Tan RG. Detection of lymph node metastases in head and neck cancer: a meta-analysis comparing US, USgFNAC, CT and MR imaging. Eur J Radiol. 2007 Nov;64(2):266-72. DOI: 10.1016/j.ejrad.2007.02.037

93. de Bondt RB, Nelemans PJ, Bakers F, Casselman JW, Peutz-Kootstra C, Kremer B, Hofman PA, Beets-Tan RG. Morphological MRI criteria improve the detection of lymph node metastases in head and neck squamous cell carcinoma: multivariate logistic regression analysis of MRI features of cervical lymph nodes. Eur Radiol. 2009 Mar;19(3):626-33. DOI: 10.1007/s00330-008-1187-3

94. Bisdas S, Baghi M, Huebner F, Mueller C, Knecht R, Vorbuchner M, Ruff J, Gstoettner W, Vogl TJ. In vivo proton MR spectroscopy of primary tumours, nodal and recurrent disease of the extracranial head and neck. Eur Radiol. 2007 Jan;17(1):251-7. DOI: 10.1007/s00330-006-0294-2

95. Chawla S, Kim S, Loevner LA, Quon H, Wang S, Mutale F, Weinstein G, Delikatny EJ, Poptani H. Proton and phosphorous MR spectroscopy in squamous cell carcinomas of the head and neck. Acad Radiol. 2009 Nov;16(11):1366-72. DOI: 10.1016/j.acra.2009.06.001

96. Abdel Razek AA, Gaballa G. Role of perfusion magnetic resonance imaging in cervical lymphadenopathy. J Comput Assist Tomogr. 2011 Jan-Feb;35(1):21-5. DOI: 10.1097/RCT.0b013e3181ff9143

97. Harisinghani MG, Barentsz J, Hahn PF, Deserno WM, Tabatabaei S, van de Kaa CH, de la Rosette J, Weissleder R. Noninvasive detection of clinically occult lymph-node metastases in prostate cancer. N Engl J Med. 2003 Jun 19;348(25):2491-9. DOI: 10.1056/NEJMoa022749

98. Sigal R, Vogl T, Casselman J, Moulin G, Veillon F, Hermans R, Dubrulle F, Viala J, Bosq J, Mack M, Depondt M, Mattelaer C, Petit P, Champsaur P, Riehm S, Dadashitazehozi Y, de Jaegere T, Marchal G, Chevalier D, Lemaitre L, Kubiak C, Helmberger R, Halimi P. Lymph node metastases from head and neck squamous cell carcinoma: MR imaging with ultrasmall superparamagnetic iron oxide particles (Sinerem MR) – results of a phase-III multicenter clinical trial. Eur Radiol. 2002 May;12(5):1104-13. DOI: 10.1007/s003300101130

99. Baghi M, Mack MG, Wagenblast J, Hambek M, Rieger J, Bisdas S, Gstoettner W, Engels K, Vogl T, Knecht R. Iron oxide particle-enhanced magnetic resonance imaging for detection of benign lymph nodes in the head and neck: how reliable are the results? Anticancer Res. 2007 Sep-Oct;27(5B):3571-5.

100. Mack MG, Balzer JO, Straub R, Eichler K, Vogl TJ. Superparamagnetic iron oxide-enhanced MR imaging of head and neck lymph nodes. Radiology. 2002 Jan;222(1):239-44. DOI: 10.1148/radiol.2221010225

101. Herborn CU, Lauenstein TC, Vogt FM, Lauffer RB, Debatin JF, Ruehm SG. Interstitial MR lymphography with MS-325: characterization of normal and tumor-invaded lymph nodes in a rabbit model. AJR Am J Roentgenol. 2002 Dec;179(6):1567-72.

102. Lambregts DM, Beets GL, Maas M, Kessels AG, Bakers FC, Cappendijk VC, Engelen SM, Lahaye MJ, de Bruïne AP, Lammering G, Leiner T, Verwoerd JL, Wildberger JE, Beets-Tan RG. Accuracy of gadofosveset-enhanced MRI for nodal staging and restaging in rectal cancer. Ann Surg. 2011 Mar;253(3):539-45. DOI: 10.1097/SLA.0b013e31820b01f1

103. Vandecaveye V, De Keyzer F, Dirix P, Lambrecht M, Nuyts S, Hermans R. Applications of diffusion-weighted magnetic resonance imaging in head and neck squamous cell carcinoma. Neuroradiology. 2010 Sep;52(9):773-84. DOI: 10.1007/s00234-010-0743-0

104. Abdel Razek AA, Kandeel AY, Soliman N, El-shenshawy HM, Kamel Y, Nada N, Denewar A. Role of diffusion-weighted echo-planar MR imaging in differentiation of residual or recurrent head and neck tumors and posttreatment changes. AJNR Am J Neuroradiol. 2007 Jun-Jul;28(6):1146-52. DOI: 10.3174/ajnr.A0491

105. Vandecaveye V, De Keyzer F, Nuyts S, Deraedt K, Dirix P, Hamaekers P, Vander Poorten V, Delaere P, Hermans R. Detection of head and neck squamous cell carcinoma with diffusion weighted MRI after (chemo)radiotherapy: correlation between radiologic and histopathologic findings. Int J Radiat Oncol Biol Phys. 2007 Mar 15;67(4):960-71. DOI: 10.1016/j.ijrobp.2006.09.020

106. Re TJ, Lemke A, Klauss M, Laun FB, Simon D, Grünberg K, Delorme S, Grenacher L, Manfredi R, Mucelli RP, Stieltjes B. Enhancing pancreatic adenocarcinoma delineation in diffusion derived intravoxel incoherent motion f-maps through automatic vessel and duct segmentation. Magn Reson Med. 2011 Nov;66(5):1327-32. DOI: 10.1002/mrm.22931

107. Dirix P, Vandecaveye V, De Keyzer F, Op de Beeck K, Poorten VV, Delaere P, Verbeken E, Hermans R, Nuyts S. Diffusion-weighted MRI for nodal staging of head and neck squamous cell carcinoma: impact on radiotherapy planning. Int J Radiat Oncol Biol Phys. 2010 Mar 1;76(3):761-6. DOI: 10.1016/j.ijrobp.2009.02.068

108. Sumi M, Sakihama N, Sumi T, Morikawa M, Uetani M, Kabasawa H, Shigeno K, Hayashi K, Takahashi H, Nakamura T. Discrimination of metastatic cervical lymph nodes with diffusion-weighted MR imaging in patients with head and neck cancer. AJNR Am J Neuroradiol. 2003 Sep;24(8):1627-34.

109. Sumi M, Van Cauteren M, Nakamura T. MR microimaging of benign and malignant nodes in the neck. AJR Am J Roentgenol. 2006 Mar;186(3):749-57. DOI: 10.2214/AJR.04.1832

110. Knegjens JL, Hauptmann M, Pameijer FA, Balm AJ, Hoebers FJ, de Bois JA, Kaanders JH, van Herpen CM, Verhoef CG, Wijers OB, Wiggenraad RG, Buter J, Rasch CR. Tumor volume as prognostic factor in chemoradiation for advanced head and neck cancer. Head Neck. 2011 Mar;33(3):375-82.

111. Bhatia KS, King AD, Yu KH, Vlantis AC, Tse GM, Mo FK, Ahuja AT. Does primary tumour volumetry performed early in the course of definitive concomitant chemoradiotherapy for head and neck squamous cell carcinoma improve prediction of primary site outcome? Br J Radiol. 2010 Nov;83(995):964-70. DOI: 10.1259/bjr/27631720

112. Jansen JF, Schöder H, Lee NY, Stambuk HE, Wang Y, Fury MG, Patel SG, Pfister DG, Shah JP, Koutcher JA, Shukla-Dave A. Tumor metabolism and perfusion in head and neck squamous cell carcinoma: pretreatment multimodality imaging with 1H magnetic resonance spectroscopy, dynamic contrast-enhanced MRI, and [18F]FDG-PET. Int J Radiat Oncol Biol Phys. 2012 Jan 1;82(1):299-307. DOI: 10.1016/j.ijrobp.2010.11.022

113. Chawla S, Kim S, Loevner LA, Hwang WT, Weinstein G, Chalian A, Quon H, Poptani H. Prediction of disease-free survival in patients with squamous cell carcinomas of the head and neck using dynamic contrast-enhanced MR imaging. AJNR Am J Neuroradiol. 2011 Apr;32(4):778-84. DOI: 10.3174/ajnr.A2376

114. Kim S, Loevner LA, Quon H, Kilger A, Sherman E, Weinstein G, Chalian A, Poptani H. Prediction of response to chemoradiation therapy in squamous cell carcinomas of the head and neck using dynamic contrast-enhanced MR imaging. AJNR Am J Neuroradiol. 2010 Feb;31(2):262-8. DOI: 10.3174/ajnr.A1817

115. Herborn CU, Unkel C, Vogt FM, Massing S, Lauenstein TC, Neumann A. Whole-body MRI for staging patients with head and neck squamous cell carcinoma. Acta Otolaryngol. 2005 Nov;125(11):1224-9. DOI: 10.1080/00016480510040128

116. Antoch G, Vogt FM, Freudenberg LS, Nazaradeh F, Goehde SC, Barkhausen J, Dahmen G, Bockisch A, Debatin JF, Ruehm SG. Whole-body dual-modality PET/CT and whole-body MRI for tumor staging in oncology. JAMA. 2003 Dec 24;290(24):3199-206. DOI: 10.1001/jama.290.24.3199

117. Schmidt GP, Baur-Melnyk A, Herzog P, Schmid R, Tiling R, Schmidt M, Reiser MF, Schoenberg SO. High-resolution whole-body magnetic resonance image tumor staging with the use of parallel imaging versus dual-modality positron emission tomography-computed tomography: experience on a 32-channel system. Invest Radiol. 2005 Dec;40(12):743-53. DOI: 10.1097/01.rli.0000185878.61270.b0

118. Schmidt GP, Schoenberg SO, Schmid R, Stahl R, Tiling R, Becker CR, Reiser MF, Baur-Melnyk A. Screening for bone metastases: whole-body MRI using a 32-channel system versus dual-modality PET-CT. Eur Radiol. 2007 Apr;17(4):939-49. DOI: 10.1007/s00330-006-0361-8

119. Ng SH, Chan SC, Yen TC, Liao CT, Chang JT, Ko SF, Wang HM, Lin CY, Chang KP, Lin YC. Comprehensive imaging of residual/recurrent nasopharyngeal carcinoma using whole-body MRI at 3 T compared with FDG-PET-CT. Eur Radiol. 2010 Sep;20(9):2229-40. DOI: 10.1007/s00330-010-1784-9

120. Liu T, Cheng T, Xu W, Yan WL, Liu J, Yang HL. A meta-analysis of 18FDG-PET, MRI and bone scintigraphy for diagnosis of bone metastases in patients with breast cancer. Skeletal Radiol. 2011 May;40(5):523-31. DOI: 10.1007/s00256-010-0963-8

121. Ohno Y, Koyama H, Onishi Y, Takenaka D, Nogami M, Yoshikawa T, Matsumoto S, Kotani Y, Sugimura K. Non-small cell lung cancer: whole-body MR examination for M-stage assessment – utility for whole-body diffusion-weighted imaging compared with integrated FDG PET/CT. Radiology. 2008 Aug;248(2):643-54. DOI: 10.1148/radiol.2482072039

122. Weckbach S, Michaely HJ, Stemmer A, Schoenberg SO, Dinter DJ. Comparison of a new whole-body continuous-table-movement protocol versus a standard whole-body MR protocol for the assessment of multiple myeloma. Eur Radiol. 2010 Dec;20(12):2907-16. DOI: 10.1007/s00330-010-1865-9

123. Fischer M, Strauß G, Gahr S, Richter I, Müller S, Burgert O, Dornheim J, Preim B, Dietz A, Boehm A. Dreidimensionale Bildprozessierung in der HNO-Onkologie zur präoperativen Planung und Evaluierung. Laryngo-Rhino-Otol. 2009;88:229-33. DOI: 10.1055/s-0029-1202815

124. Kösling S, Bootz F. Bildgebung HNO-Heilkunde. Springer-Verlag; 2010.

125. Aschenbach R, Eßer D. Bildgebung in der HNO. Laryngo-Rhino-Otol. 2011;90:103-18. DOI: 10.1055/s-0030-1270561

126. Stuck BA, Bachert C, Federspil P, Hörmann K, Hosemann W, Klimek L, Mösges R, Pfaar O, Rudack C, Wagenmann M, Weber R. AWMF Leitlinie der Deutschen Gesellschaft für Hals-Nasen-Ohren-Heilkunde, Kopf- und Hals-Chirurgie. Rhinosinusitis. Langfassung. AWMF-Leitlinienregister Nr. 017/049; aktueller Stand: 03/2011

127. Zinreich SJ, Kennedy DW, Rosenbaum AE, Gayler BW, Kumar AJ, Stammberger H. Paranasal sinuses: CT imaging requirements for endoscopic surgery. Radiology. 1987 Jun;163(3):769-75.

128. Dammann F. Bildgebung der Nasennebenhohlen (NNH) in der heutigen Zeit. Radiologe. 2007;47:576, 578-83. DOI: 10.1007/s00117-007-1502-z

129. AWMF Leitlinien der Deutschen Röntgengesellschaft. Gesichtsschädel. Entzündungen. AWMF Leitlinienregister Nr. 039/037.

130. Lang S, Jager L, Grevers G. Zur Aussagefähigkeit koronarer Sekundärrekonstruktionen computertomographischer Sequenzen der Nasenneben-höhlen. Laryngo-Rhino-Otol. 2002;81:418-21. DOI: 10.1055/s-2002-32212

131. Dammann F, Bode A, Heuschmid M, Kopp A, Georg C, Pereira PL, Claussen CD. Mehrschicht-Spiral-CT der Nasennebenhöhlen: Erste Erfahrungen unter besonderer Berücksichtigung der Strahlenexposition [Multislice spiral CT of the paranasal sinuses: first experiences using various parameters of radiation dosage]. Rofo. 2000 Aug;172(8):701-6. DOI: 10.1055/s-2000-7175

132. Strauss G, Meixensberger J, Dietz A, Manzey D. Automation in der HNO-Chirurgie [Automation in surgery: a systematical approach]. Laryngorhinootologie. 2007 Apr;86(4):256-62. DOI: 10.1055/s-2007-966296

133. Salvolini L, Bichi Secchi E, Costarelli L, De Nicola M. Clinical applications of 2D and 3D CT imaging of the airways – a review. Eur J Radiol. 2000 Apr;34(1):9-25. DOI: 10.1016/S0720-048X(00)00155-8

134. Cattin P, Schulz G, Reyes M. Bildgebende Verfahren. Neue Methoden verändern die Chirurgie. MKG-Chirurg. 2011;4:16-22. DOI: 10.1007/s12285-010-0195-x

135. Moharir VM, Fried MP, Vernick DM, Janecka IP, Zahajsky J, Hsu L, Lorensen WE, Anderson M, Wells WM, Morrison P, Kikinis R. Computer-assisted three-dimensional reconstruction of head and neck tumors. Laryngoscope. 1998 Nov;108(11 Pt 1):1592-8. DOI: 10.1097/00005537-199811000-00002

136. Rudman DT, Stredney D, Sessanna D, Yagel R, Crawfis R, Heskamp D, Edmond CV Jr,Wiet GJ. Functional endoscopic sinus surgery training simulator. Laryngoscope. 1998 Nov;108(11 Pt 1):1643-7. DOI: 10.1097/00005537-199811000-00010

137. Stasche N, Quirrenbach T, Bärmann M, Krebs M, Harrass M, Friedrich K. IMOLA – ein interventionsfähiges Larynxmodell. Ausbildung in der transoralen Lasermikrochirurgie der oberen Atemwege [IMOLA – a new larynx model for surgical training. Education in transoral laser microsurgery of the upper airways]. HNO. 2005 Oct;53(10):869-72, 874-5. DOI: 10.1007/s00106-005-1309-z

138. Holzapfel K, Duetsch S, Fauser C, Eiber M, Rummeny EJ, Gaa J. Value of diffusion-weighted MR imaging in the differentiation between benign and malignant cervical lymph nodes. Eur J Radiol. 2009 Dec;72(3):381-7. DOI: 10.1016/j.ejrad.2008.09.034

139. de Bondt RB, Hoeberigs MC, Nelemans PJ, Deserno WM, Peutz-Kootstra C, Kremer B, Beets-Tan RG. Diagnostic accuracy and additional value of diffusion-weighted imaging for discrimination of malignant cervical lymph nodes in head and neck squamous cell carcinoma. Neuroradiology. 2009 Mar;51(3):183-92. DOI: 10.1007/s00234-008-0487-2

140. Abdel Razek AA, Soliman NY, Elkhamary S, Alsharaway MK, Tawfik A. Role of diffusion-weighted MR imaging in cervical lymphadenopathy. Eur Radiol. 2006 Jul;16(7):1468-77. DOI: 10.1007/s00330-005-0133-x

141. Perrone A, Guerrisi P, Izzo L, D'Angeli I, Sassi S, Mele LL, Marini M, Mazza D, Marini M. Diffusion-weighted MRI in cervical lymph nodes: differentiation between benign and malignant lesions. Eur J Radiol. 2011 Feb;77(2):281-6. DOI: 10.1016/j.ejrad.2009.07.039

142. Vandecaveye V, Dirix P, De Keyzer F, Op de Beeck K, Vander Poorten V, Hauben E, Lambrecht M, Nuyts S, Hermans R. Diffusion-weighted magnetic resonance imaging early after chemoradiotherapy to monitor treatment response in head-and-neck squamous cell carcinoma. Int J Radiat Oncol Biol Phys. 2012 Mar 1;82(3):1098-107. DOI: 10.1016/j.ijrobp.2011.02.044

143. Berrak S, Chawla S, Kim S, Quon H, Sherman E, Loevner LA, Poptani H. Diffusion weighted imaging in predicting progression free survival in patients with squamous cell carcinomas of the head and neck treated with induction chemotherapy. Acad Radiol. 2011 Oct;18(10):1225-32. DOI: 10.1016/j.acra.2011.06.009

144. Kim S, Loevner L, Quon H, Sherman E, Weinstein G, Kilger A, Poptani H. Diffusion-weighted magnetic resonance imaging for predicting and detecting early response to chemoradiation therapy of squamous cell carcinomas of the head and neck. Clin Cancer Res. 2009 Feb 1;15(3):986-94. DOI: 10.1158/1078-0432.CCR-08-1287

145. Vandecaveye V, Dirix P, De Keyzer F, de Beeck KO, Vander Poorten V, Roebben I, Nuyts S, Hermans R. Predictive value of diffusion-weighted magnetic resonance imaging during chemoradiotherapy for head and neck squamous cell carcinoma. Eur Radiol. 2010 Jul;20(7):1703-14. DOI: 10.1007/s00330-010-1734-6

146. King AD, Mo FK, Yu KH, Yeung DK, Zhou H, Bhatia KS, Tse GM, Vlantis AC, Wong JK, Ahuja AT. Squamous cell carcinoma of the head and neck: diffusion-weighted MR imaging for prediction and monitoring of treatment response. Eur Radiol. 2010 Sep;20(9):2213-20. DOI: 10.1007/s00330-010-1769-8

Corresponding author:
Prof. Dr. med. Maliha Sadick
Institute of Clinical Radiology and Nuclear Medicine, University Hospital Mannheim, Medical Faculty Mannheim of the University of Heidelberg, Theodor Kutzer Ufer 1-3, 68167 Mannheim, Germany
maliha.sadick@umm.de

Please cite as
Sadick M, Schoenberg SO, Hoermann K, Sadick H. Current oncologic concepts and emerging techniques for imaging of head and neck squamous cell cancer. GMS Curr Top Otorhinolaryngol Head Neck Surg. 2012;11:Doc08.
DOI: 10.3205/cto000090, URN: urn:nbn:de:0183-cto0000903

This article is freely available from
http://www.egms.de/en/journals/cto/2012-11/cto000090.shtml

Published: *2012-12-20*